AFML-TR-65-56
PART II

ULTRASONIC STUDIES OF THE NONLINEAR PROPERTIES AND OF THE DEFORMATION OF SOLIDS

AKIRA HIKATA — FRANK A. SEWELL, JR.
BRUCE B. CHICK — CHARLES ELBAUM

BROWN UNIVERSITY

FOREWORD

This report was prepared by the Metals Research Laboratory, Division of Applied Mathematics, Brown University, Providence, Rhode Island, under USAF Contract No. AF33(657)-8324. This contract was initiated under Project No. 7360, "The Chemistry and Physics of Materials", Task No. 736002, "Nondestructive Methods". The work was administered under the direction of the AF Materials Laboratory, Research and Technology Division, with Mr. W. L. Shelton, MAMD, acting as the project engineer.

This report covers work conducted from January 1, 1965 to December 31, 1965, and is a continuation of work done under Contract No. AF33(616)-6945. This report was submitted on January 28, 1966.

We are indebted to Mr. Richard Rowand for direct assistance and for encouragement in connection with this work.

This technical report has been reviewed and is approved.

W. J. TRAPP
Chief, Strength and Dynamics Branch
Metals and Ceramics Division
Air Force Materials Laboratory

ABSTRACT

This report is concerned with a continuation (see report for 1964[1]) of the research on the nonlinear properties of solids, with special emphasis on the role of dislocations in harmonic generation, the effects of plastic deformation and dislocation interactions with point defects.

An expanded and improved theory of harmonic generation has been developed. The main new features of this theory include: 1) A demonstration that, in the string model, the nonlinear behavior of screw and edge dislocations is qualitatively and quantitatively different. In particular, it is shown that the nonlinear terms responsible for harmonic generation are of opposite sign for the two cases; edge dislocations behave as "hardening" strings and screw dislocations as "softening" strings. 2) The contributions of the lattice and of dislocations to the amplitude of the second harmonic are difficult to separate when the two are of comparable magnitude.

Dislocation breakaway from pinning points was considered as a possible source of harmonic generation; this contribution is of the same sign as that from screw dislocations.

Experiments were carried out on aluminum single crystals with several different impurity contents, as measured by electrical resistivity ratios ($R_{300^\circ k}/R_{4.2^\circ k}$) ranging from 270 to 3100. Amplitudes of the third harmonic, as well as the attenuation of the fundamental wave, were measured as a function of bias stress, amplitude of the fundamental wave and amount of plastic deformation. The results of these experiments are consistent with the qualitative predictions of the theory presented.

A capacitive pick-up method was used to measure the magnitude of the fundamental and higher harmonic amplitudes for the purpose of comparison with the quantitative aspects of the theory.

TABLE OF CONTENTS

ILLUSTRATIONS

ILLUSTRATIONS

I. Introduction

This report is concerned with research on the physics of deformation and its application to the study of defects in solids. The particular aspects of this study covered in the past year are: 1) non-linear behavior of solids due to the vibrational motion of dislocations; 2) the separation of dislocation and lattice contributions to the non-linear behavior; 3) experimental studies of the influence of controllable parameters, such as impurity content and amount of plastic deformation, on the properties mentioned.

The general background of the research discussed in the following was presented at some length in the "End of the Year" Report for 1964[1], and will not be repeated here in detail. A few of the calculations that appeared in that report have been extended and repeated here, for ease of reference and to maintain continuity. The remainder of the material is new.

The study consists in calculating and measuring the distortion, or harmonic generation, of waves propagating in metal single crystals.

When a sinusoidal ultrasonic wave of a given frequency and of sufficient amplitude is introduced into a nonlinear or anharmonic solid, the fundamental wave will distort as it propagates, so that the second, the third and higher harmonics of the fundamental frequency will be generated. In many solids the nonlinearity of the stress-strain relation (deviation from Hooke's law) may arise from two causes. One is the anharmonicity of the lattice, which is a characteristic of all solids, and the other is the contribution of the non-linear part of the stress-strain relation for dislocation displacement; this cause applies to solids in which glide motion of dislocations is produced by small stresses, i.e., to most metals. The remainder of this discussion refers to the cases for which both contributions are present.

The dislocation contribution to the generation of second harmonics in high purity aluminum single crystals was demonstrated by Hikata et al.[1)2)3)] It should be emphasized here, however, that for the generation of the second harmonic the stress-strain relation must be nonlinear, as well as not symmetric with respect to displacement gradients. In the case of dislocations, therefore, the displacement from the equilibrium position should be different for equal positive and negative values of stress. This condition may be achieved, for example, by applying a static bias stress in addition to the ultrasonic wave, assuming that the dislocations are straight at the outset. The static bias stresses usually required for this purpose are in the range 10^5 ~ 10^6 dynes/cm^2; these stresses have no measurable effect on the coefficients of the anharmonic terms of the lattice[1)2)3)].

In the case of the third harmonic, however, the condition of nonsymmetry is not required. A symmetric (nonlinear) stress-strain relation is sufficient to generate the third harmonic; in other words, the bias stress is no longer necessary for dislocations to generate the third harmonic. In the case of the second harmonic, the absolute value of the thermal expansion coefficient is a measure of the lattice contribution[4)], and in the cases studied so far, the lattice contribution and the dislocation contribution were found to be of

comparable magnitude. Thus, in order to study experimentally either lattice or dislocation anharmonicity it is necessary to separate the two effects. On the other hand, the lattice contribution to the third harmonic is found to be a factor of ten or more smaller than the dislocation contribution to the third harmonic (the dislocation contribution is comparable for the second and the third harmonic). Therefore, by investigating the third harmonic, it should be possible to obtain detailed information on dislocation motion under stress without the complications of the lattice contribution.

In references (1) and (2), the generation of the second harmonic has been analysed on the assumption that the increase of potential energy of a dislocation is proportional to the increase of its length. Although the analysis was successful in explaining most of the experimental results, the effect that the dislocation oscillation is damped was not taken into account. Under the same assumption Suzuki et al.[5] have treated the problem using the vibrating string analogy for dislocations and have incorporated the effect of dislocation damping on the amplitude of the second harmonic generated in the specimen. In the following analysis, the latter treatment is extended to the case of the third harmonic with some modifications and refinements.

II. Theory of Second and Third Harmonics in String Approximation.

Equation of Motion

When a stress wave is propagated along a solid containing dislocations, the dislocations will oscillate causing additional local displacement and strain in the solid. If one denotes the longitudinal displacement of an infinitesimal element of a solid in the x-direction by u, then

$$u = u_\ell + u_d$$

where u_ℓ is the displacement of the lattice, and u_d is the displacement due to the dislocation motion. The one-dimensional form of the equation of motion for the displacement u in the x-direction is given by

$$\rho \frac{\partial^2 u}{\partial t^2} = \rho \frac{\partial^2}{\partial t^2}(u_\ell + u_d) = \frac{\partial \sigma}{\partial x} \tag{1}$$

where ρ is the density of the undeformed material, σ is the applied stress and t denotes time. It is convenient for us to use the differentiated form (with respect to x) of Equation (1)

$$\rho \frac{\partial^2}{\partial t^2}\left(\frac{\partial u_\ell}{\partial x} + \frac{\partial u_d}{\partial x}\right) = \frac{\partial^2 \sigma}{\partial x^2} \tag{2}$$

Thus, the problem is now reduced to expressing $\frac{\partial u_\ell}{\partial x}$ and $\frac{\partial u_d}{\partial x}$ as a function of stress σ and to solve the Equation (2) with respect to σ. In the present case, however, a sinusoidal wave of frequency ω is introduced at one end of the specimen (at x = 0). As the wave propagates, the wave form will be distorted due to the nonlinearity of the solid. Therefore, at a distance x, the stress σ should be expressed in terms of the harmonics of the fundamental wave, i.e.,

$$\begin{aligned}\sigma = A_o + A_1 \cos(\omega t - kx) + A_2 \cos 2(\omega t - kx - \delta_2) \\ + A_3 \cos 3(\omega t - kx - \delta_3) + ...\end{aligned} \tag{3}$$

where A_o is a static bias stress, A_1, A_2, A_3 ..... are the amplitudes of the fundamental, the second and the third and higher harmonic waves respectively, $2\delta_2$ and $3\delta_3$..... are the phase angles of the second and the third and higher harmonics relative to the fundamental wave respectively, and k is the wave vector. It is assumed here that dispersion is negligible. For purposes of actual calculations, terms beyond the third harmonic in Equation (3) are not used.

The boundary conditions are:

at $x = 0$,

$$A_1 = A_{10} \text{ (the amplitude of the induced fundamental wave)}$$

$$A_2 = A_3 = 0$$

Since the nonlinearity considered here is not expected to be large, one can assume that

$$A_2, A_3 \ll A_1$$

Thus, if one expresses both sides of Equation (2) in terms of the harmonics, a comparison of the sine and cosine terms of the corresponding frequencies will provide sets of equations which determine the amplitudes of the harmonics.

Expression for $\frac{\partial u_\ell}{\partial x}$

The one-dimensional relation between stress σ and displacement-gradient $\frac{\partial u_\ell}{\partial x}$ of a solid, correct to the square terms is given by[6)]

$$\sigma = E_1 \frac{\partial u_\ell}{\partial x} + a\left(\frac{\partial u_\ell}{\partial x}\right)^2 \tag{4}$$

where E_1 is the second order elastic constant and a is a combination of the second and the third order elastic constants.

Thus,

(continued next page)

$$\frac{\partial u_\ell}{\partial x} = \frac{1}{E_1}\sigma - \frac{a}{E_1^3}\sigma^2 + \ldots .$$

$$= \frac{A_o}{E_1} - \frac{a}{E_1^3}\left(A_o^2 + \frac{A_1^2}{2}\right)$$

$$+ \left[\frac{A_1}{E_1} - \frac{a}{E_1^3}\left(2A_oA_1 + A_1A_2\cos 2\delta_2\right)\right]\cos(\omega t - kx)$$

$$- \left[\frac{a}{E_1^3}A_1A_2\sin 2\delta_2\right]\sin(\omega t - kx)$$

$$+ \left[\frac{A_2}{E_1}\cos 2\delta_2 - \frac{a}{E_1^3}\left(2A_oA_2\cos 2\delta_2 + \frac{A_1^2}{2}\right)\right]\cos 2(\omega t - kx) \qquad (5)$$

$$+ \left[\frac{A_2}{E_1}\sin 2\delta_2 - \frac{a}{E_1^3}2A_oA_2\sin 2\delta_2\right]\sin 2(\omega t - kx)$$

$$+ \left[\frac{A_3}{E_1}\cos 3\delta_3 - \frac{a}{E_1^3}\left(2A_oA_3\cos 3\delta_3 + A_1A_2\cos 2\delta_2\right)\right]\cos 3(\omega t - kx)$$

$$+ \left[\frac{A_3}{E_1}\sin 3\delta_3 - \frac{a}{E_1^3}\left(2A_oA_3\sin 3\delta_3 + A_1A_2\sin 2\delta_2\right)\right]\sin 3(\omega t - kx)$$

Expression for $\frac{\partial u_d}{\partial x}$

The linear case of small amplitude dislocation oscillations under the influence of an externally applied oscillatory stress was treated, using the string analogy, by Koehler[7] and later by Granato and Lücke[8]. In these treatments (7), (8), the line energy is assumed to be independent of the position and orientation of a dislocation. In fact, however, even in an isotropic material, the line energy of an edge dislocation differs significantly from that of a screw dislocation[9][10][11][12]. It follows that, in general, the line energy of a bowed out dislocation (under an external stress) is not constant along the dislocation line. In the case of an anisotropic solid, the energy difference between edge and screw dislocations could be quite large as pointed out by Foreman[10], and deWit and Koehler[11].

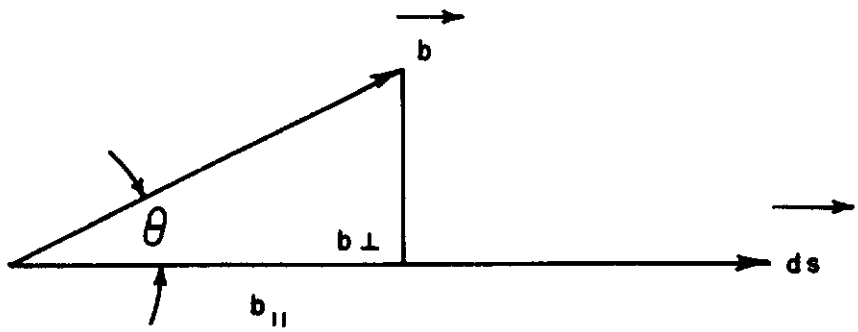

Figure 2. Relation between Burgens Vector $\vec{b}$ and the Dislocation Line Segment $\vec{ds}$.

taken as the $\xi\eta$ plane and the dislocation line is defined by $\xi = f(\eta)$ Fig. 1). Then, by using Equation (8) the following is obtained:

$$V = \int d\eta W_e \left[\sqrt{1 + f'^2} \{1 - m \cos^2(\theta - \theta')\} - (1 - m \cos^2\theta) \right]$$

Here, $f' = \partial\xi/\partial\eta$, and $\theta - \theta' = \theta$ is the angle between the line segment and Burgers vector, and the meaning of θ and θ' is explained in Fig. 1. Introducing $\tan\theta' = f'$ we obtain

$$V = \int d\eta W_e \left[\sqrt{1 + f'^2} \left\{1 - \frac{m}{1 + f'^2} (\cos^2\theta + 2f' \sin\theta \cos\theta + f'^2 \sin^2\theta)\right\} - (1 - m \cos^2\theta) \right] \tag{10}$$

The integrand of (10) can be expanded in powers of f'. If one keeps terms up to the fourth power in f', the result is given by

$$V = \int d\eta W_e \left[- 2m f' \sin\theta \cos\theta + \frac{1}{2} (1 + m \cos^2\theta - 2m \sin^2\theta) f'^2 + f'^3 \sin\theta \cos\theta - \frac{1}{8} (1 + 3m \cos^2\theta - 4m \sin^2\theta) f'^4 \right] \tag{11}$$

If the dislocation is pinned at $\eta = 0$ and $\eta = L$, the deviations from the straight configuration should be the same for equal positive and negative stresses. In other words, V should be symmetrical in terms of f'. Therefore, in Equation (11) the terms containing f' and f'^3 should vanish.

The equilibrium condition for the line segment L can be obtained from a variational principle; i.e., the total energy $W = V - V_\tau$ should be an extremal, where V_τ is the work done by the external force and given by

$$V_\tau = \tau b \int_0^L f(\eta)\, d\eta \quad ,$$

τ; resolved shear stress in the glide plane and in the slip direction.

The equilibrium condition becomes

$$\delta W = \delta(V - V_\tau) = 0 \quad ,$$

or, according to the Euler-Lagrange equation,

$$\frac{d}{d\eta} \frac{\partial W}{\partial f'} - \frac{\partial W}{\partial f} = 0$$

The result is then

$$- f''W_e\left[(1 + m\cos^2\theta - 2m\sin^2\theta) - \frac{3}{2}(1 + 3m\cos^2\theta - 4m\sin^2\theta)f'^2\right] = \tau b \qquad (12)$$

If one assumes that the line energies of edge dislocations and of screw dislocations are equal, i.e., m = 0, then Equation (12) becomes

$$- W_e f''(1 - \frac{3}{2} f'^2) = \tau b \ ,$$

which is the case treated in references (1), (2), (3), (5). If one assumes further that the higher order term is negligible, the equation reduces to

$$- W_e f'' = \tau b \ ,$$

which is the case of the linear approximation treated by Granato and Lücke[8]. Even in an isotropic material, m is not equal to zero, and is given by

$$m = \nu = 1/3 \qquad (\nu: \text{ Poisson's ratio}).$$

Thus, for an edge dislocation ($\theta = \pi/2$), Equation (12) reduces to

$$- \frac{1}{3} W_e f''(1 + \frac{3}{2} f'^2) = \tau b$$

or, since $\frac{W_e}{3} \simeq \frac{1}{2}\mu b^2$,

$$- \frac{1}{2} b^2 f''(1 + \frac{3}{2} f'^2) = \tau b \qquad (13)$$

For a screw dislocation ($\theta = 0$) ,

$$\begin{aligned} &- \frac{4}{3} W_e f''(1 - \frac{9}{4} f'^2) = \tau b \\ &- 2\mu b^2 f''(1 - \frac{9}{4} f'^2) = \tau b \ . \end{aligned} \qquad (14)$$

Equations (13) and (14) reveal two important features:

a) The linear term of Equation (13), $- (1/2)\mu b^2 f''$, is 1/4 of the linear term of Equation (14), $- 2\mu b^2 f''$. This means that for a small applied stress, the displacement of an edge dislocation is approximately four times larger than that of a screw dislocation. Therefore, for a small oscillatory stress, it is expected that the contribution from edge dislocations is predominant for the quantities such as attenuation and velocity change, provided that the density and loop length of the two types of the dislocations are similar.

b) The nonlinear term in Equation (13), $- (3/2)f'^2$ is negative, while that of

Equation (14), + (9/4) f'^2 is positive. This means that the stress-displacement relation for edge dislocations is hardening (as the applied stress increases, a larger stress increment is necessary to produce a given amount of displacement), while the stress-displacement relation for screw dislocations is softening (see Fig. 3). Of course, the deviation from a linear stress-displacement relationship, whether it is softening or hardening, is the source of the harmonic generation.

The nonlinear relation between a static stress and the dislocation displacement of a pinned dislocation leads to the following equation of motion of a dislocation under the influence of combined static and oscillatory stresses:

$$A \frac{\partial^2 \xi}{\partial t^2} + B \frac{\partial \xi}{\partial t} - C \left[\left(\frac{\partial^2 \xi}{\partial \eta^2}\right) - C' \left(\frac{\partial \xi}{\partial \eta}\right)^2 \left(\frac{\partial^2 \xi}{\partial \eta^2}\right)\right] = bR\sigma \qquad (15)$$

where

σ is given by Equation (3)

$A = \pi \rho b^2$ (effective mass of dislocation per unit length),

B = damping coefficient,

$C = W_e (1 + m \cos^2\theta - 2m \sin^2\theta)$,

$$C' = \frac{3}{2} \frac{(1 + 3m \cos^2\theta - 4m \sin^2\theta)}{(1 + m \cos^2\theta - 2m \sin^2\theta)},$$

m and θ are the quantities defined in the previous section,

b = Burgers vector,

R = resolving shear factor converting the axial stress to the shear stress in the slip plane and in the slip direction.

The terms $A\frac{\partial^2 \xi}{\partial t^2}$ and $B\frac{\partial \xi}{\partial t}$ represent the inertia force and frictional force of a dislocation per unit length respectively. The nonlinear differential Equation (15) can be solved approximately by iteration. First, utilizing the Fourier expansion of $bR\sigma$, one obtains a solution ξ_1 for the linear approximation of Equation (15) (i.e., the equation without the nonlinear term),

$$\xi_1 = \xi_{10} + \xi_{11} + \xi_{12} + \xi_{13}, \qquad (16)$$

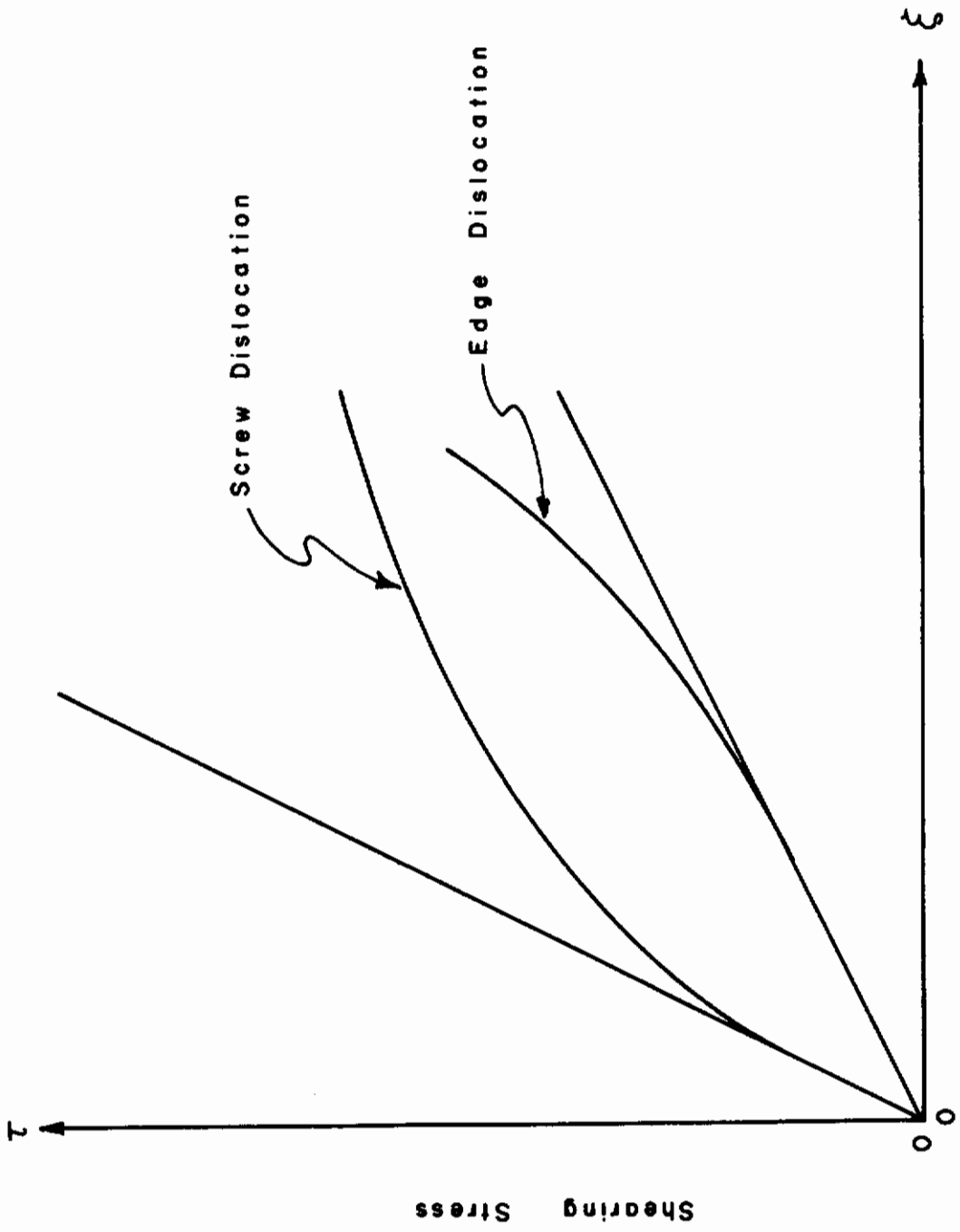

Figure 3. Stress-Displacement Diagram of Edge and Screw Dislocations (schematic).

where

$$\xi_{10} = \frac{4bRA_o L_o^2}{\pi^3 C} \sum_o^\infty \frac{1}{(2n+1)^3} \sin\frac{(2n+1)\pi\eta}{L_o}$$

$$\xi_{11} = \frac{4bRA_1}{A\pi} \sum^\infty \frac{1}{2n+1} \frac{1}{S_n^{1/2}} \sin\frac{(2n+1)\pi\eta}{L_o} \cos(\omega\tau - kx - \delta_{1n})$$

with

$$S_n = (\omega_n^2 - \omega^2)^2 + (\omega d)^2 \ ,$$

$$\omega_n = (2n+1)\frac{\pi}{L_o}\left(\frac{C}{A}\right)^{1/2} \ ,$$

$$\tan\delta_{1n} = \frac{\omega d}{\omega_n^2 - \omega^2} \ ,$$

$$d = \frac{B}{A} \ ,$$

$$\xi_{12} = \frac{4bRA_2}{A\pi} \sum_o^\infty \frac{1}{2n+1} \frac{1}{M_n^{1/2}} \sin\frac{(2n+1)\pi\eta}{L_o} \cos 2(\omega t - kx - \delta_2 - \delta_{2n})$$

with;

$$M_n = \{\omega_n^2 - (2\omega)^2\}^2 + (2\omega d)^2 \ ,$$

$$\tan 2\delta_{2n} = \frac{2\omega d}{\omega_n^2 - (2\omega)^2} \ ,$$

$$\xi_{13} = \frac{4bRA_3}{A\pi} \sum_o^\infty \frac{1}{2n+1} \cdot \frac{1}{T_n^{1/2}} \cdot \sin\frac{(2n+1)\pi\eta}{L_o} \cdot \cos 3(\omega t - kx - \delta_3 - \delta_{3n}),$$

with

$$T = \{\omega_n^2 - (3\omega)^2\}^2 + (3\omega d)^2 \ ,$$

$$\tan 3\delta_{3n} = \frac{3\omega d}{\omega_n^2 - \omega^2} \ .$$

In the following analysis, only the first terms (n = 0) of each infinite series are taken into account[13]. Inserting $\xi = \xi_1 + \xi_2$ into Equation (15), where ξ_2 is the iterated solution, and retaining those nonlinear terms containing only ξ_1, one obtains the equation

$$A \frac{\partial^2 \xi_2}{\partial t^2} + B \frac{\partial \xi_2}{\partial t} - C \frac{\partial^2 \xi_2}{\partial \eta^2} = - CC' \left(\frac{\partial \xi_1}{\partial \eta}\right)^2 \left(\frac{\partial^2 \xi_1}{\partial \eta^2}\right)$$

$$= \frac{CC'}{4} \left(\frac{\pi}{L_o}\right)^4 \left(\sin\frac{3\pi\eta}{L_o} + \sin\frac{\pi\eta}{L_o}\right) x$$

$$\{A_o P + A_1 Q \cos(\omega t - kx - \delta_{10}) + A_2 K \cos 2(\omega t - kx - \delta_2 - \delta_{20}) \tag{17}$$

$$+ A_3 J \cos 3(\omega t - kx - \delta_3 - \delta_{30})\}^3 ,$$

where

$$P = \frac{4bRL_o^2}{\pi^3 C} , \quad Q = \frac{4bR}{A\pi S_o^{1/2}} , \quad K = \frac{4bR}{A\pi M_o^{1/2}} ,$$

and

$$J = \frac{4bR}{A\pi T_o^{1/2}} .$$

Neglecting the term $\sin\frac{3\pi\eta}{L_o}$[14] and retaining the terms up to the third harmonic in the right hand side of Equation (17), one obtains the solution ξ_2,

$$\xi_2 = \xi_{20} + \xi_{21} + \xi_{22} + \xi_{23} , \tag{18}$$

where

$$\xi_{20} = h \sin\frac{\pi\eta}{L_o} \frac{L^2}{\pi^2 C} \left[A_o^3 P^3 + \frac{3}{2} A_o P A_1^2 Q^2\right] ,$$

$$h = \frac{CC'}{4} \left(\frac{\pi}{L_o}\right)^4 ,$$

$$\xi_{21} = h \sin\frac{\pi\eta}{L_o} \frac{1}{AS_o^{1/2}} \left[\left\{\frac{3}{4} A_1^3 Q^3 + 3A_o^2 P^2 A_1 Q\right\}\cos(\omega t - kx - 2\delta_{10})\right.$$

$$\left. + 3A_o P A_1 Q A_2 K \cos(\omega t - kx - 2\delta_2 - 2\delta_{20})\right]$$

$$\xi_{22} = h \sin\frac{\pi\eta}{L_o} \frac{1}{AM_o^{1/2}} \left[\frac{3}{2} A_o P A_1^2 Q^2 \cos 2(\omega t - kx - \delta_{10} - \delta_{20})\right.$$

$$\left. + 3A_o^2 P^2 A_2 K \cos 2(\omega t - kx - \delta_2 - \delta_{20})\right]$$

$$\xi_{23} = h \sin\frac{\pi\eta}{L_o} \frac{1}{AT_o^{1/2}} \left[\frac{1}{4} A_1^3 Q^3 \cos 3(\omega t - kx - \delta_{10} - \delta_{30})\right.$$

$$+ 3A_o^2 P^2 A_3 J \cos 3(\omega t - kx - \delta_3 - 2\delta_{30})$$

$$\left. + 3A_o P A_1 Q A_2 K \cos 3\left(\omega t - kx - \frac{\delta_{10} + 2\delta_2 + 2\delta_{20} + 3\delta_{30}}{3}\right)\right]$$

Thus, after one iteration, one obtains for the solution of Equation (15),

$$\xi = \xi_1 + \xi_2 \ . \tag{19}$$

where ξ_1 and ξ_2 are given by expression (16) and (18).

Once ξ is obtained in terms of η, $\frac{\partial u_d}{\partial x}$ can be calculated by the following relation,

$$\frac{\partial u_d}{\partial x} = \frac{Nb\Omega}{L_o} \int_o^{L_o} \xi d\eta \tag{20}$$

where N is the effective dislocation density and Ω is a factor converting the shear strain to the longitudinal strain.

Amplitude of the Second and Third Harmonic

Inserting the expressions (3), (5) and (20) into Equation (2) and equating separately the sine and cosine terms of each harmonic, the following relations are obtained:

$$\frac{d^2A_1}{dx^2} - k^2A_1 = -\rho\omega^2\left[\frac{A_1}{E_1} - \frac{a}{E_1^3}\left(2A_oA_1 + A_1A_2\cos 2\delta_2\right) + gQA_1\cos\delta_{10}\right.$$

$$\left. + h\,g\frac{1}{AS_o^{1/2}}\left\{\left(\frac{3}{4}A_1^3Q^3 + 3A_o^2P^2A_1Q\right)\cos 2\delta_{10} + 3A_oPA_1QA_2K\cos 2(\delta_2 + \delta_{20})\right\}\right] \tag{21}$$

$$2k\frac{dA_1}{dx} = -\rho\omega^2\left[-\frac{a}{E_1^3}A_1A_2\sin 2\delta_2 + A_1Qg\sin\delta_{10} + h\frac{g}{AS_o^{1/2}}\left\{\frac{3}{4}A_1^3Q^3 + 3A_o^2P^2A_1Q\right)\sin 2\delta_{10}\right.$$

$$\left. + 3A_oPA_1QA_2K\sin 2(\delta_2 + \delta_{20})\right\}\Big] \tag{22}$$

$$\frac{d^2A_2}{dx^2}\cos 2\delta_2 - 4k\frac{dA_2}{dx}\sin 2\delta_2 - 4k^2A_2\cos 2\delta_2$$

$$= -4\rho\omega^2\left[\frac{A_2}{E_1}\cos 2\delta_2 - \frac{a}{E_1^3}\left(2A_oA_2\cos 2\delta_2 + \frac{A_1^2}{2}\right)\right.$$

$$+ A_2Kg\cos 2(\delta_2 + \delta_{20}) + h\frac{g}{AM_o^{1/2}}\left\{\frac{3}{2}A_oPA_1^2Q^2\cos 2(\delta_{10} + \delta_{20})\right.$$

$$\left.\left. + 3A_o^2P^2A_2K\cos 2(\delta_2 + 2\delta_{20})\right\}\right] \tag{23}$$

$$\frac{d^2A_2}{dx^2}\sin 2\delta_2 + 4k\frac{dA_2}{dx}\cos 2\delta_2 - 4k^2A_2\sin 2\delta_2$$

$$= -4\rho\omega^2\left[\frac{A_2}{E_1}\sin 2\delta_2 - \frac{a}{E_1^3}\left(2A_oA_2\sin 2\delta_2\right)\right.$$

$$+ KA_2g\sin 2(\delta_2 + \delta_{20}) + h\frac{g}{AM_o^{1/2}}\left\{\frac{3}{2}A_oPA_1^2Q^2\sin 2(\delta_{10} + \delta_{20})\right.$$

$$\left.\left. + 3A_o^2P^2A_2K\sin 2(\delta_2 + 2\delta_{20})\right\}\right] \tag{24}$$

$$\frac{d^2A_3}{dx^2}\cos 3\delta_3 - 6k\frac{dA_3}{dx}\sin 3\delta_3 - 9k^2A_3\cos 3\delta_3$$

$$= -9\rho\omega^2\left[\frac{A_3}{E_1}\cos 3\delta_3 - \frac{a}{E_1^3}\left(2A_oA_3\cos 3\delta_3 + A_1A_2\cos 2\delta_2\right)\right.$$

$$+ JA_3g\cos 3(\delta_3 + \delta_{30}) + h\left(\frac{g}{AT_o^{1/2}}\right)\left\{\frac{1}{4}A_1^3Q^3\cos 3(\delta_{10} + \delta_{30})\right. \qquad (25)$$

$$+ 3A_o^2P^2A_3J\cos 3(\delta_3 + 2\delta_{20})$$

$$\left.\left. + 3A_oPA_1QA_2K\cos(\delta_{10} + 2\delta_2 + 2\delta_{20} + 3\delta_{30})\right\}\right]$$

$$\frac{d^2A_3}{dx^2}\sin 3\delta_3 + 6k\frac{dA_3}{dx}\cos 3\delta_3 - 9k^2A_3\sin 3\delta_3$$

$$= -9\rho\omega^2\left[\frac{A_3}{E_1}\sin 3\delta_3 - \frac{a}{E_1^3}\left(2A_oA_3\sin 3\delta_3 + A_1A_2\sin 2\delta_2\right)\right.$$

$$+ JA_3g\sin 3(\delta_3 + \delta_{30}) + h\frac{g}{AT_o^{1/2}}\left\{\frac{1}{4}A_1^3Q^3\sin 3(\delta_{10} + \delta_{30})\right. \qquad (26)$$

$$+ 3A_o^2P^2A_3J\sin 3(\delta_3 + 2\delta_{20})$$

$$\left.\left. + 3A_oPA_1QA_2K\sin(\delta_{10} + 2\delta_2 + 2\delta_{20} + 3\delta_{30})\right\}\right]$$

where

$$g = \frac{2Nb\Omega}{\pi}\ .$$

In Equations (21) and (22), the terms containing A_2 are much smaller than the terms containing A_1; furthermore, in the present study the term containing A_1^3 is negligible compared with the term containing A_1. These terms are, therefore, neglected. After these approximations one obtains as the solutions of Equations (21) and (22),

$$A_1 = A_{10}\,e^{-\alpha_1 x} \qquad (27)$$

with

$$\alpha_1 = \frac{\rho\omega^2 g}{2k}\left[Q\sin\delta_{10} + \frac{3h}{AS_o^{1/2}}A_o^2P^2Q\sin 2\delta_{10}\right] \qquad (28)$$

$$k^2 - \alpha_1^2 = \rho\omega^2 \left[\frac{1}{E_1} - \frac{2a}{E_1^3} A_o + g \left\{Q \cos\delta_{10} + \frac{3h}{AS_o^{1/2}} A_o^2 P^2 Q \cos 2\delta_{10}\right\}\right] \quad (29)$$

where A_{10} is the amplitude of the induced oscillatory stress at x = 0.

The expression (28) represents the attenuation of the fundamental wave. Since $k = \omega/v$ and $v = \sqrt{E/\rho}$ (v is the velocity of sound in the material), the first term of the expression (28) can be written

$$\alpha_{10} = \frac{4NE_1 b^2 \Omega R \omega^2 d}{vA\pi^2 S_o} , \quad (30)$$

which agrees with Granato and Lücke's[8] results. The second term of the expression (28) represents the effect of bias stress on the attenuation. Although it increases with the square of the bias stress, its contribution to the attenuation turns out to be negligible in the stress range of interest here.

From Equation (29), one can derive the velocity change of $\Delta v/v$ of the fundamental wave,

$$\frac{\Delta v}{v} \cong \frac{a}{E_1^2} A_o - 1/2E_1 g\{Q \cos\delta_{10} + \frac{3h}{AS_o^{1/2}} A_o^2 P^2 Q \cos 2\delta_{10}\}. \quad (31)$$

From Equations (23) and (24), the amplitude A_2 of the second harmonic can be obtained;

$$A_2 = \{\frac{a}{2E_1^3} \sin 2\delta_2 - \frac{3}{2} \frac{h \cdot g}{AM_o^{1/2}} A_o P Q^2 \sin 2(\delta_2 - \delta_{10} - \delta_{20})\} \frac{\rho\omega^2}{k} \cdot A_{10}^2 \cdot \frac{e^{-2\alpha_1 x} - e^{-\alpha_2 x}}{\alpha_2 - 2\alpha_1} \quad (32)$$

with;

$$\alpha_2 = \frac{\rho\omega^2 g}{k} \{K \sin 2\delta_{20} + \frac{3h}{AM_o^{1/2}} A_o^2 P^2 K \sin 4\delta_{20}\} , \quad (33)$$

where the following relation should also be satisfied,

$$\frac{d^2A_2}{dx^2} = [4k^2 - 4\rho\omega^2 \{\frac{1}{E_1} - \frac{2a}{E_1^3} A_o + Kg \cos 2\delta_{20}$$

$$+ \frac{3hg}{AM_o^{1/2}} A_o^2 P^2 K \cos 4\delta_{20}\}] A_2 \qquad (34)$$

$$+ 4\rho\omega^2 \{\frac{a}{2E_1^3} \cos 2\delta_2 - \frac{3}{2} \frac{h \cdot g}{AM_o^{1/2}} A_o PQ^2 \cos 2(\delta_2 - \delta_{10} - \delta_{20})\} A_1$$

If one compares the expression for α_2 (Equation (33)) and that of the fundamental wave α_1 (Equation (28)), it is easily seen that α_2 is equivalent to the attenuation of an independent wave propagating with a frequency 2ω. This means that since dispersion is assumed to be negligible, the following relation between k and α_2 should also hold,

$$4k^2 - \alpha_2^2 = 4\rho\omega^2 [\frac{1}{E_1} - \frac{2a}{E_1^3} A_o + g \{K \cos 2\delta_{20} + \frac{3h}{AM_o^{1/2}} A_o^2 P^2 K \cos 4\delta_{20}\}] \qquad (35)$$

Substituting the expressions (32) and (35) into (34), one obtains the following relation for the phase angle δ_2 between the fundamental and the second harmonic

$$\tan 2\delta_2 \cong \frac{\frac{a}{2E_1} - \frac{3h}{AM_o^{1/2}} A_o PQ^2 \cos 2(\delta_{10} + \delta_{20})}{\frac{3h}{AM_o^{1/2}} A_o PQ^2 \sin 2(\delta_{10} + \delta_{20})} \qquad (36)$$

If one neglects the dislocation contribution to the second harmonic, the phase angle becomes,

$$2\delta_2 = \frac{\pi}{2} .$$

On the other hand, if one neglects the lattice contribution, $2(\delta_2 - \delta_{10} - \delta_{20})$ is very close to $\frac{\pi}{2}$. Thus, one can express the amplitude of the second harmonic with reasonable accuracy as follows,

$$A_2 = \frac{\rho\omega^2}{k} [X^2 + Y^2 - 2XY \cos 2(\delta_{10} + \delta_{20})]^{1/2} \cdot A_{10}^2 \cdot \frac{e^{-2\alpha_1 x} - e^{-\alpha_2 x}}{\alpha_2 - 2\alpha_1} \qquad (37)$$

where

$$X = \frac{a}{2E_1^3}$$

$$Y = \frac{48Nb^4R^3\Omega C'A_o}{\pi^2 A^3 S_o M_o^{1/2} L_o^2} \quad ,$$

furthermore, in the case where $\omega_o >> 4\omega$, the factor

$$\cos 2(\delta_{10} + \delta_{20})$$

can be replaced by

$$\frac{\omega_o^2}{S_o M_o^{1/2}} (\omega_o^4 - 5\omega^2 d^2)$$

From Equations (25) and (26), the following expressions for the amplitude A_3 and the attenuation α_3 of the third harmonic can be obtained:

$$A_3 = \frac{3}{8} \frac{\rho\omega^2 g}{k} \frac{h Q^3 A_{10}^3 \sin 3(\delta_3 - \delta_{10} - \delta_{30})}{AT_o^{1/2}} \cdot \frac{e^{-3\alpha_1 x} - e^{-\alpha_3 x}}{\alpha_3 - 3\alpha_1} \tag{38}$$

$$\alpha_3 = \frac{3}{2} \frac{\rho\omega^2 g}{k} \{J \sin 3\delta_{30} + \frac{3h}{AT_o^{1/2}} A_o^2 P^2 J \sin 6\delta_{30}\} \quad , \tag{39}$$

where the following relation should also be satisfied,

$$\frac{d^2 A_3}{dx^2} = [9k^2 - 9\rho\omega^2 \{\frac{1}{E_1} - \frac{2a}{E_1^3} A_o + g(J \cos 3\delta_{30} + \frac{3h}{AT_o^{1/2}} A_o^2 P^2 J \cos 6\delta_{30})\}] A_3 \tag{40}$$

$$- [\frac{9}{4} \rho\omega^2 \frac{g \cdot h}{AT_o^{1/2}} Q^3 \cos 3(\delta_3 - \delta_{10} - \delta_{30})] A_1^3$$

As in the case of the second harmonic, expression (39) indicates that the third harmonic generated in the solid attenuates in the same manner as an independent wave of frequency 3ω introduced into the solid. This leads to the following condition determining the phase angle $3\delta_3$ between the fundamental and the third harmonic wave,

$$\tan 3(\delta_3 - \delta_{10} - \delta_{30}) = \frac{6k}{\alpha_3 + 3\alpha_1}$$

Since the right hand side of the above equation is a very large quantity, $3(\delta_3 - \delta_{10} - \delta_{30})$ is positive and very close to $\frac{\pi}{2}$. Thus, one can express the amplitude of the third harmonic with reasonable accuracy as follows:

$$A_3 = \frac{12\rho\omega^2 Nb^4 \Omega R^3 CC' A_{10}^3}{kA^4 S_o^{3/2} T_o^{1/2} L_o^4} \cdot \frac{e^{-3\alpha_1 x} - e^{-\alpha_3 x}}{\alpha_3 - 3\alpha_1} \qquad (41)$$

It should be emphasized that expression (41) represents the contribution of dislocations only to the third harmonic and that the lattice contribution is neglected.

Discussion

In the following, several significant consequences of the above expressions are presented.

a) There are two contributions to the second harmonic, one arising from the lattice anharmonicity which is represented by the first term of the expression (37); the other arising from the nonlinear dislocation motion which is represented by the second term of the expression. In addition, the existence of the phase angle $2(\delta_{10} + \delta_{20})$ between the two components leads to the cross term in expression (37). The factor Y is a function of dislocation density, of bias stress (internal or external) and of loop length (which in turn depends on bias stress), while X is independent of the bias stresses in the range considered here and is a constant for a given solid and mode of wave propagation. In general, a separation of the two contributions is quite difficult because of the cross term in expression (37). Under certain circumstances, either X or Y is dominant and the cross term is unimportant. A separation of the two terms is also possible, of course, when $2(\delta_{10} + \delta_{20}) \approx \frac{\pi}{2}$ (δ_{10} and δ_{20} depend on loop length).

In the case of the third harmonic, the lattice contribution does not appear in the expression (41). This is simply because the terms in powers higher than the square of the displacement-gradient are not taken into account in the expression (4). Although for the lattice part the magnitude of the cubic term relative to the linear and the square terms is not known at present, it is reasonable to assume that in most solids the lattice contribution to the third harmonic is negligible, at least near room temperature, where the temperature dependence of the thermal expansion coefficient is small. Thus, the third harmonic observable near room temperature can be considered to be predominantly due to the nonlinear motion of dislocations.

b) The amplitudes of the second and third harmonic are proportional respectively to the square and cube of the amplitude of the fundamental wave as long as the dislocation loop lengths remain constant.

c) At x = 0, the amplitude of the harmonics is zero. As the fundamental wave propagates along the x-axis, it starts generating the harmonics. However, both fundamental and harmonic waves suffer attenuation. The resulting initial build-up followed by a decay of the amplitude of the second and third harmonics as a function of propagation distance x are represented respectively by

$$\frac{e^{-2\alpha_1 x} - e^{-\alpha_2 x}}{\alpha_2 - 2\alpha_1} \tag{42}$$

and

$$\frac{e^{-3\alpha_1 x} - e^{-\alpha_3 x}}{\alpha_3 - 3\alpha_1} \tag{43}$$

Each factor has a maximum at a distance $(x_2)_{max}$ and $(x_3)_{max}$ given by the following relations

$$(x_2)_{max} = \frac{\log_e \frac{2\alpha_1}{\alpha_2}}{2\alpha_1 - \alpha_2} \quad (cm) \tag{44}$$

$$(x_3)_{max} = \frac{\log_e \frac{3\alpha_1}{\alpha_3}}{3\alpha_1 - \alpha_3} \quad (cm) \tag{45}$$

d) Since C appears in the factors S_o, M_o and T_o, the magnitude and the sign of the harmonics depend on the values of C and C', which are, of course, a function of the orientation angle θ. In Figure 4, the factors

$$\beta = \frac{C}{W_e} = 1 + m - 3m \sin^2\theta$$

and

$$C' = \frac{3}{2} \frac{(1 + 3m - 7m \sin^2\theta)}{(1 + m - 3m \sin^2\theta)}$$

are plotted as a function of θ, taking $m = \nu = \frac{1}{3}$ (ν is Poisson's ratio). As can be seen, C' changes its sign at approximately $\theta = 67.5$ degrees. This means that the harmonics generated by the dislocations whose orientation angles (see Figure 4) are in the range $0 < \theta < 67.5$ degrees are opposite in sign to the harmonics generated by the dislocations whose orientation angles are in the

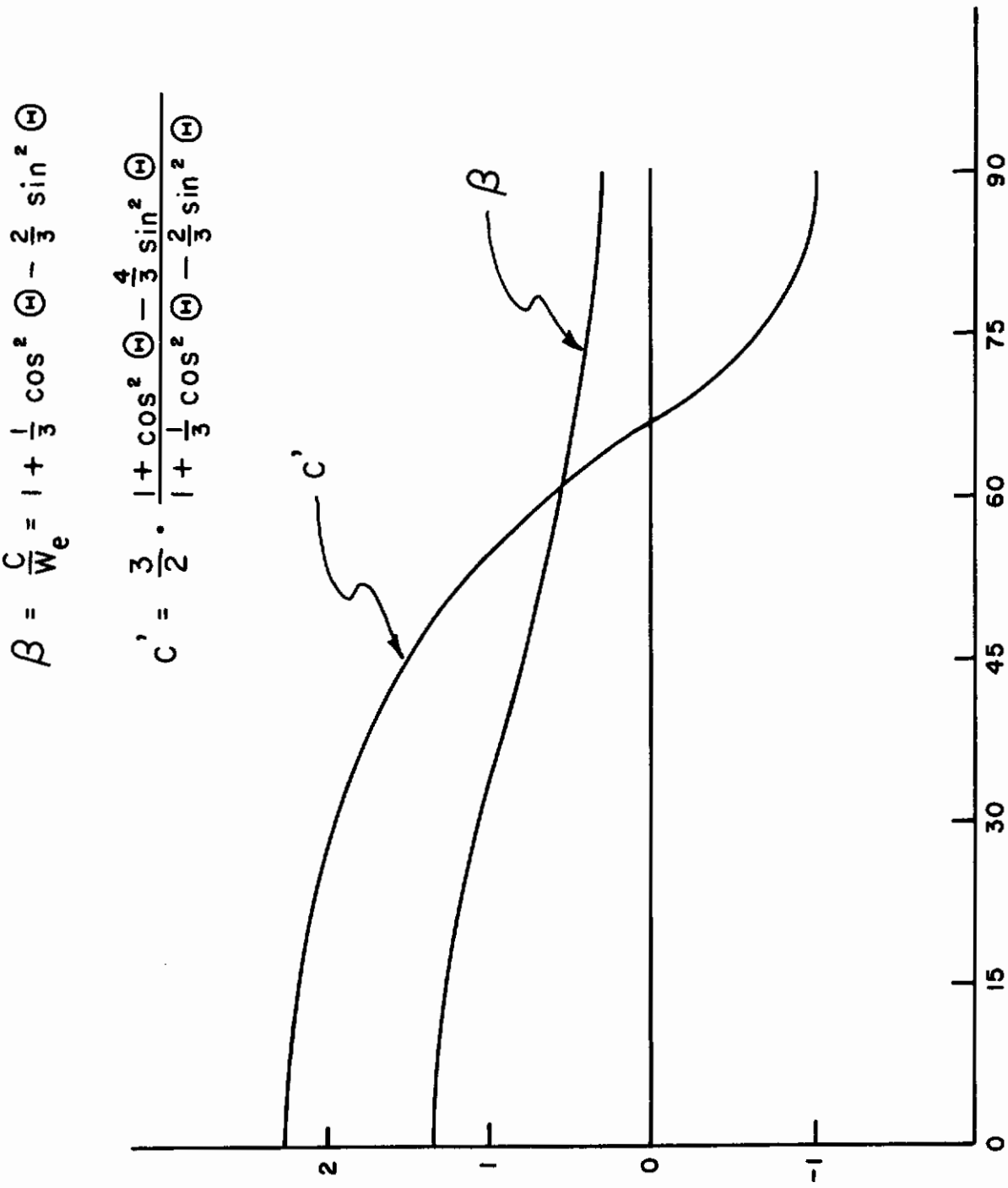

Figure 4. Factors β' and C' as a Function of Orientation Angle Θ.

range $67.5^{\circ} < \theta < 90^{\circ}$. In the case of the second harmonic, the applied static stress A_o is, in fact, a parameter to indicate the degree of deviation of a bowed out dislocation from its straight line configuration. Therefore, whether the static stress is tension or compression, the absolute value $|A_o|$ should be used in evaluating the expression (37). Thus, except for the factor C', the quantities that appear in the dislocation contribution are all positive. The contribution of the dislocations may be of the same or opposite sign as the lattice term, depending on the relative signs of X and Y, as well as on the sign of $(\omega_o^4 - 5\omega^2 d^2)$ - see Equation (37).

In the case of the third harmonic, the absolute value should be used in evaluating the expression (41).

The factor β (as well as C) also depends on the angle θ. The larger the value of C, the smaller is the corresponding dislocation displacement for a given stress, as discussed in the previous section. Since the amplitude of the harmonics depends strongly on the dislocation displacement, it is expected that the dislocations with smaller C values will generate larger harmonics, if other factors are identical.

In all cases the dislocation contribution depends not only on loop length but also on orientation, i.e., the angle θ. Therefore, the expression (41) should be calculated using appropriate distributions of both dislocation orientation and loop length. Since the information on the distribution of orientation and loop length is very scarce, in the following, the θ and loop length dependent part of the amplitude A_3 (disregarding the attenuation factor)

$$\frac{CC'}{S_o^{3/2} T_o^{1/2} L_o^4} \tag{46}$$

is calculated numerically for edge, screw and $\pi/3$ dislocations as a function of loop length L_o, assuming a delta function distribution at each value of loop length, and using the following values,

$A = 7.6 \times 10^{-15}$ g cm^{-1}, $B = 5 \times 10^{-4}$ dynes sec cm^{-2}, $\omega = 2\pi \times 10^{7}$ sec^{-1},

$W_e = 1.2\mu b^2$, $\mu = 3 \times 10^{11}$ dynes cm^{-2}, $b = 3 \times 10^{-8}$ cm.

The results are given in Figure 5. As can be seen, the maximum amplitude of the third harmonic arising from edge dislocations is considerably larger than that arising from screw or $\pi/3$ dislocations. In this figure, the attenuation of the fundamental wave α_1 is also plotted for the three types of dislocations. In each case, the loop length for the maximum amplitude of the third harmonic coincides approximately with the loop length corresponding to the inflection point in the attenuation curve. The maximum of the third harmonic, therefore, corresponds approximately to the transition between underdamped and overdamped behavior. The condition determining the loop length for the maximum amplitude

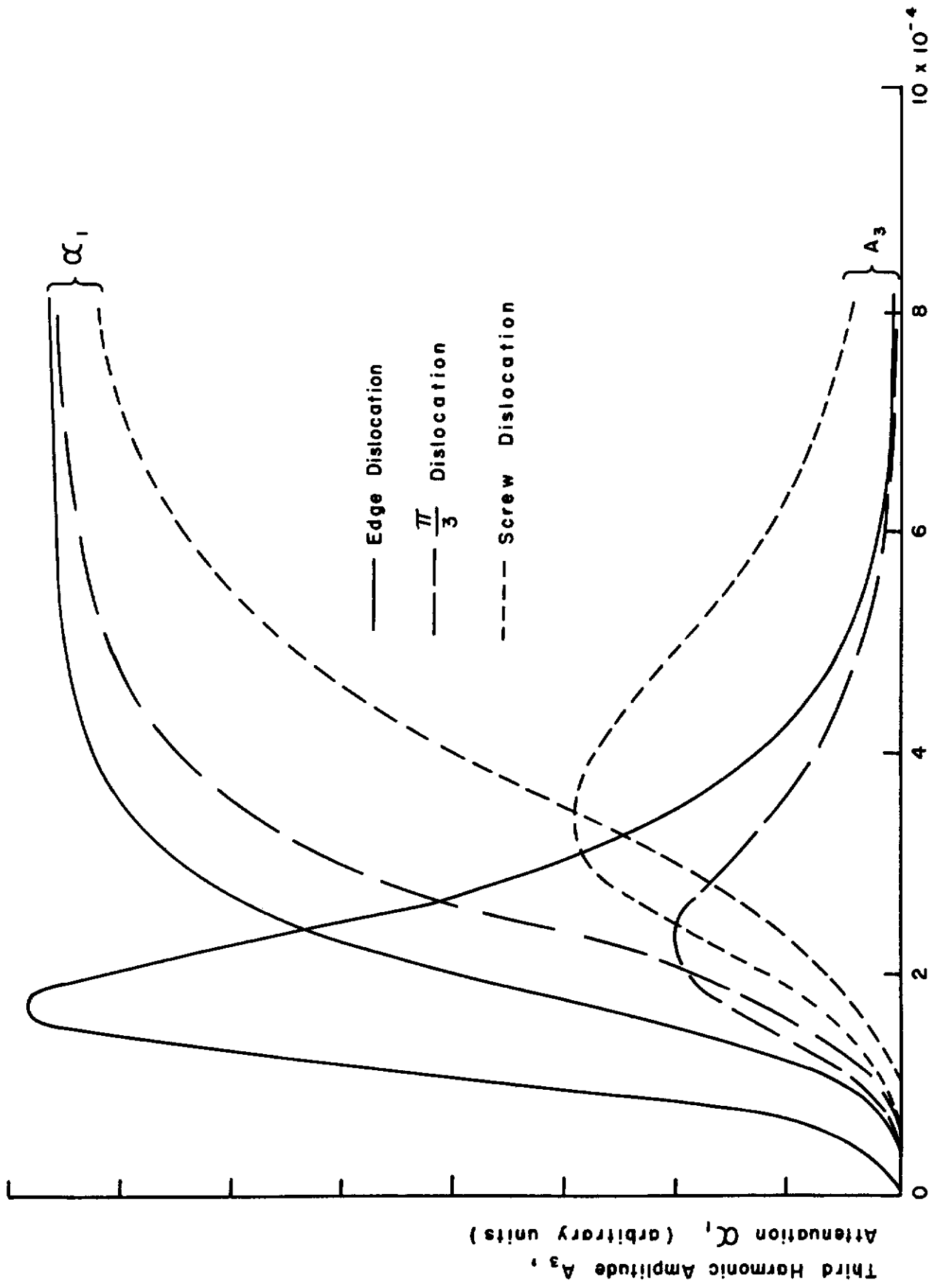

Figure 5. Amplitude of the Third Harmonic and Attenuation of the Fundamental Wave for Edge, $\pi/3$ and Screw Dislocations as a Function of Dislocation Loop Length.

A_3 is given by

$$\frac{\omega_o}{\omega} \simeq 1.12\left(\frac{d}{\omega}\right)^{1/2} \tag{47}$$

In plotting Figure 5, the absolute values are taken for the third harmonic amplitude A_3. As mentioned earlier, the amplitude A_3 for dislocations whose orientation angles θ are in the range $0 < \theta < 67.5^o$ is opposite in sign to those whose orientation angles are in the range $67.5^o < \theta < 90^o$. Therefore, cancellations of amplitude A_3 will take place when the dislocations in the two ranges operate simultaneously. To see this effect, a simple average of the expression (46) over the range $0 \leq \theta \leq 90^o$ was calculated as a function of loop length using the same numerical values as given above. The results are shown in Figure 6. The cancellation occurs approximately at the loop length of 1.9×10^{-4}cm. Whether this effect becomes significant or not depends, of course, on the orientation distribution of dislocations.

In view of the difficulties in separating the lattice and dislocation contributions in the case of the second harmonic, dislocation dynamics are studied more easily through the generation of third harmonics. It should also be emphasized that in order to study lattice anharmonicity by means of second harmonic generation, it is necessary to eliminate the dislocation contribution.

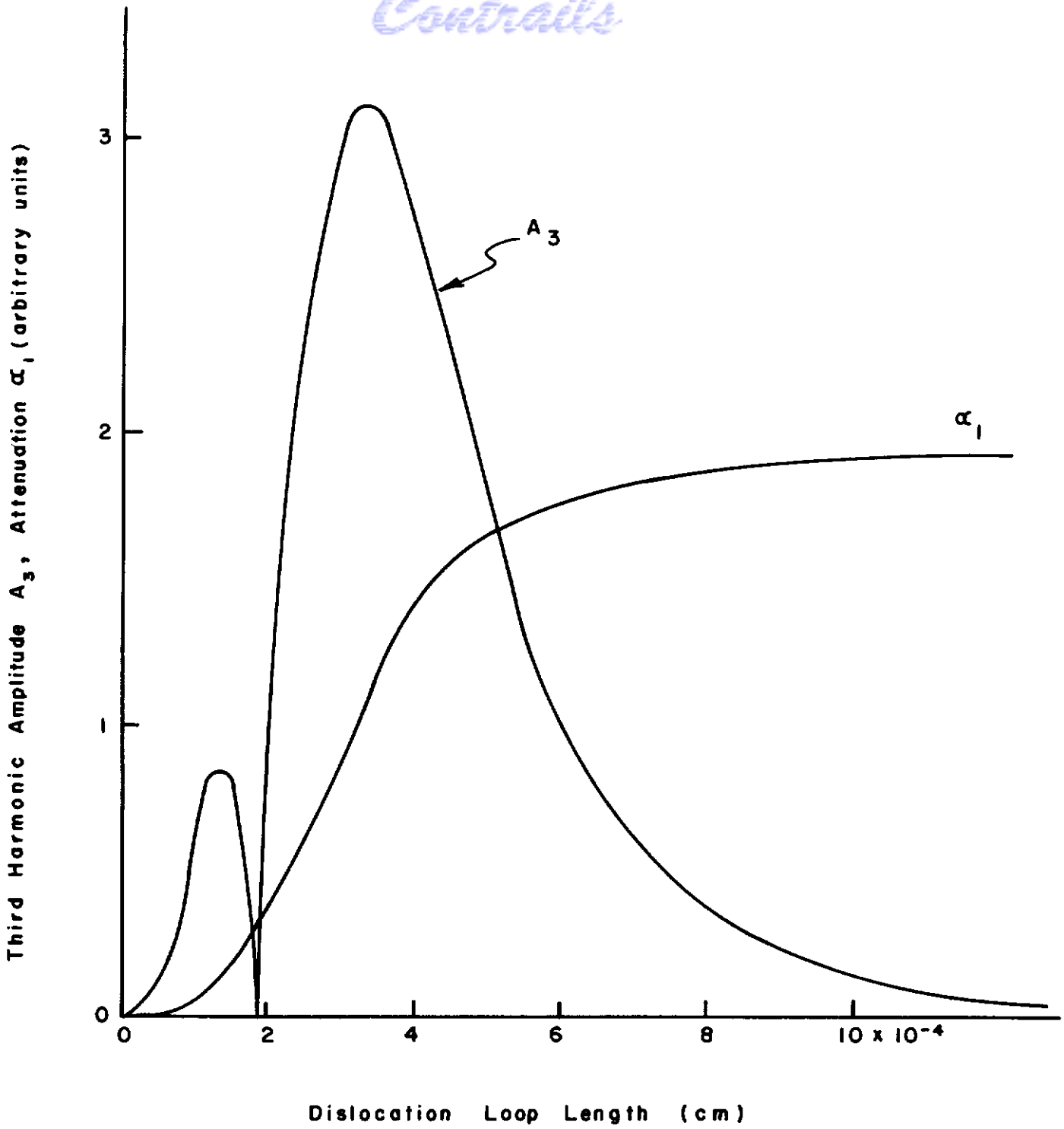

Figure 6. Amplitude of the Third Harmonic and Attenuation of the Fundamental Wave, average over the angle θ, as a Function of Dislocation Loop Length.

III. Generation of Harmonics due to Breakaway Processes

In the preceding treatment (vibrating string model), it is assumed that the loop length does not change during the course of a cycle of the oscillatory stress; i.e., the loop length is affected only by the static bias stress applied in addition to the ultrasonic stress. This assumption is valid when the amplitude of the ultrasonic wave is small so that the dislocation does not break away from the pinning points. When the amplitude of the ultrasonic wave becomes large, the dislocation will break away from weak pinning points and a change in loop length during the course of a cycle will take place, causing additional strain. This breakaway process could be nonlinear, and, therefore, be a source of harmonic generation. An analytical basis for this consideration is given in the following, though it is not complete.

The basic equations for this problem are the same as the ones that appear in the case of the nonlinear vibrating string model, i.e., the wave Equation (2) and the equation of motion of a pinned dislocation (15). To simplify the problem, we neglect the lattice anharmonicity so that the term $\frac{\partial u_\ell}{\partial x}$ can be expressed by

$$\frac{\partial u_\ell}{\partial x} = \frac{\sigma}{E} \tag{48}$$

where E is the second order elastic constant.

We neglect further the nonlinear term in the equation of motion, i.e., the term containing C'. This is equivalent to considering the nonlinearity associated with the breakaway process to be independent of the string nonlinearity. Therefore, for the purposes of this approximation one may consider that if there is no change in the loop length distribution during the stress cycle of the wave imposed on the system, the amplitude of the wave simply decreases exponentially as it propagates along the crystal, and no harmonics are generated. In such a case, the displacement gradient for the dislocation can be expressed by

$$\frac{\partial u_d}{\partial x} = b \int_o^\infty N(\ell) \int_o^\ell \xi(\eta) d\eta \, d\ell \tag{49}$$

where ξ is the solution of the equation of motion (15); and $N(\ell)$ is the distribution function of dislocation loop length, which is independent of the applied oscillatory stress σ.

If, however, a breakaway of dislocations from weak pinning points takes place during the course of a cycle, the distribution function is no longer independent of the stress. In other words, the distribution function becomes a function of time, and the time derivative $(\partial^2/\partial t^2)$ in Equation (2) may not be taken out of the integral sign. Moreover, $N(\ell)$ has a different form for

the increasing quarter cycle of stress from that which it has for the decreasing quarter cycle. Thus, the stress-dislocation strain law becomes nonlinear, and the basic Equations (2) and (15) are seen to be a system of two simultaneous nonlinear partial differential integral equations for σ and ξ in the variables x, η and t.

According to Granato and Lücke[8], the distribution function for the case when a breakaway process occurs during the cycle is given by

$$N(\ell,\sigma) = \begin{cases} N_1(\ell)d\ell = \begin{cases} \frac{\Lambda}{L_c^2}\left[1 - n\left(\frac{\tau}{\sigma} + 1\right) e^{-\frac{\tau}{\sigma}}\right] e^{-\frac{\ell}{L_c}} d\ell, & o < \ell < \mathcal{L} \\ \Lambda \frac{\delta(\ell - L_N)}{L_N} n\left(\frac{\tau}{\sigma} + 1\right) e^{-\frac{\tau}{\sigma}} d\ell, & \mathcal{L} < \ell < \infty \end{cases} \\ N_2(\ell)d\ell = \begin{cases} \frac{\Lambda}{L_c^2}\left[1 - n\left(\frac{\tau}{A_1} + 1\right) e^{-\frac{\tau}{A_1}}\right] e^{-\frac{\ell}{L_c}} d\ell, & o < \ell < \mathcal{L} \\ \Lambda \frac{\delta(\ell - L_N)}{L_N} \cdot n\left(\frac{\tau}{A_1} + 1\right) e^{-\frac{\tau}{A_1}} d\ell, & \mathcal{L} < \ell < \infty \end{cases} \end{cases} \tag{50}$$

where $N_1(\ell)d\ell$ is the distribution function for the quarter cycle of increasing stress,

$N_2(\ell)d\ell$ is the distribution function for the quarter cycle of decreasing stress.

L_c: dislocation loop length between pinning points.

L_N: dislocation network loop length.

$\sigma = A_1(x) \cdot \cos(\omega t - kx)$,

$$\tau = \frac{\pi f_m}{4bL_c} ,$$

$$f_m = \frac{3\sqrt{3}}{8} \frac{A_{int}}{y^2} ,$$

$$A_{int} = \frac{4}{3} \frac{1 + \nu}{1 - \nu} \cdot \mu b \varepsilon r_o^3 ,$$

$$\varepsilon = \frac{r_1 - r_o}{r_o} \quad ,$$

r_o, r_1: radius of the solvent and solute atoms respectively ,

ν: Poisson's ratio

n: number of loop lengths in the network. The average value of n is

$$\frac{L_N}{L_c} - 1 \quad .$$

For low stress amplitudes, where $N(\ell,\sigma)$ is independent of time, it is possible to obtain a solution to the Equations (2) and (15) in the form of an exponentially damped sinusoidal wave for σ.

$$\sigma = A_1 \cos(\omega t - kx) \quad ,$$

$$\xi = \frac{4bA_1}{\pi A} \sum_o^\infty \frac{1}{(2n+1)} \frac{1}{S_n^{1/2}} \cdot \sin\frac{(2n+1)\pi n}{L_o} \cdot \cos(\omega t - kx - \delta_{1n})$$

where

$$S_n = (\omega_n^2 - \omega^2)^2 + (\omega d)^2 \quad , \qquad (51)$$

$$\omega_n = (2n+1)\frac{\pi}{L_o}\left(\frac{C}{A}\right)^{1/2} \quad ,$$

$$\tan\delta_{1n} = \frac{\omega d}{\omega_n^2 - \omega^2} \quad , \quad d = \frac{B}{A} \quad .$$

If breakaway is included and such a trial solution for σ is used, it is found that the system (2), (15) cannot strictly be satisfied, and therefore exponentially damped sinusoidal waves of the form (51) do not constitute a complete solution. However, for low stress amplitudes, we know this to be the form of the solution and we may try to find a more complete solution, assuming the contribution of breakaway to be a perturbation. Thus, in Equation (15), we use the following expression for σ

$$\sigma = A_1(x) \cos(\omega t - kx) + A_3 \cos 3(\omega t - kx - \delta_3) \qquad (52)$$

to obtain an expression for ξ, $(A_1 > > A_3)$. Neglecting the terms $n > 1$ in the expansion one obtains

$$\xi = \frac{4bA_1}{A} \frac{1}{S_o^{1/2}} \sin\frac{\pi\eta}{L_o} \cdot \cos(\omega t - kx - \delta_{10})$$

$$+ \frac{4bA_3}{A} \frac{1}{T_o^{1/2}} \cdot \sin\frac{\pi\eta}{L_o} \cos 3(\omega t - kx - \delta_3 - \delta_{30})$$

with $T_o = \{\omega_o^2 - (3\omega)^2\}^2 + (3\omega d)^2$

$$\tan 3\delta_{30} = \frac{3\omega d}{\omega_o^2 - \omega^2} \cdot$$

Then, for the expression $\frac{\partial u_d}{\partial x}$, one obtains

$$\frac{\partial u_d}{\partial x} = \frac{8\, A_1(x)\, b^2}{\pi^4 C} \int_o^\infty \frac{N(\ell)\ell^3 \cos(\omega t - kx - \delta_{10})}{[(1 - \Omega^2)^2 + \Omega^2/D^2]^{1/2}}\, d\ell$$

$$+ \frac{8\, A_3(x)\, b^2}{\pi^4 C} \int_o^\infty \frac{N(\ell)\ell^3 \cos 3(\omega t - kx - \delta_3 - \delta_{30})}{[(1 - \Omega'^2)^2 + \frac{\Omega'^2}{D^2}]^{1/2}}\, d\ell$$

where

$$\Omega = \frac{\omega}{\omega_o} \quad \text{and} \quad D = \frac{\omega_o}{d}, \quad \Omega' = \frac{3\omega}{\omega_o}$$

For the underdamped case, we can assume that $\Omega, \Omega' << 1$, and the denominator of the integral may be replaced by unity. The cosine terms may be written as

$$\cos(\omega t - kx) + \delta_{10} \sin(\omega t - kx), \text{ and } \cos 3(\omega t - kx - \delta_3)$$

$$+ 3\delta_{30} \sin 3(\omega t - kx - \delta_3) .$$

where

$$\delta_{10} \simeq \frac{\omega d}{\beta^2} \ell^2, \quad \beta^2 = \pi^2 \frac{C}{A} = \omega_o^2 \ell^2, \quad 3\delta_{30} \simeq \frac{3\omega d}{\beta^2} \ell^2$$

The dynamic phase angles are used here even though we are interested in phase variations over the course of a quarter cycle, since the transients have a relaxation time constant which is several powers of 10 smaller than a period. Therefore, the transients are damped out in a negligible fraction of the quarter period and the dynamic phase angle obtains.

With the above substitutions, Equation (49) becomes

$$\frac{\partial u_d}{\partial x} = \frac{8\, A_1(x)\, b^2}{\pi^4 C} \int_0^\infty N(\ell)\ell^3 \left[\cos(\omega t - kx) + \frac{\omega d}{\beta^2}\ell^2 \sin(\omega t - kx)\right] d\ell$$

$$+ \frac{8\, A_3(x)\, b^2}{\pi^4 C} \int_0^\infty N(\ell)\ell^3 \left[\cos 3(\omega t - kx - \delta_3) + \frac{3\omega d}{\beta^2}\ell^2 \sin 3(\omega t - kx - \delta_3)\right] d\ell$$

For the first quarter cycle of increasing stress,

$$\int_0^\infty N(\ell)\ell^3\, d\ell = \Lambda L_c^2\, 3!\, \left[1 + \frac{\gamma^3}{3!}\frac{\tau}{\sigma} e^{-\frac{\tau}{\sigma}}\right]$$

$$\int_0^\infty N(\ell)\ell^5\, d\ell = L_c^4\, 5!\, \left[1 + \frac{\gamma^5}{5!}\frac{\tau}{\sigma} e^{-\frac{\tau}{\sigma}}\right] .$$

For the second quarter cycle, one needs only replace

$$\sigma = A_1(x) \cos(\omega t - kx)$$

by $A_1(x)$ in the above expression.

Here, $\gamma = \frac{L_N}{L_c}$.

Thus, $\frac{\partial u_d}{\partial x}$ is the sum of a cosine and a sine term in $(\omega t - kx)$ for each quarter cycle. The variation of $\frac{\partial u_d}{\partial x}$ for the cosine term over the course of a cycle is shown in Figure 7a. For the decreasing quarter cycle, the function is purely sinusoidal, whereas for the next quarter cycle, it is sinusoidal at first, but then increases swiftly to a maximum value.

$\frac{\partial u_d}{\partial x}$ may be written in the form

$$\frac{\partial u_d}{\partial x} = \begin{cases} F_1 \cos\theta + G_1 \sin\theta + F_3 \cos 3\theta + G_3 \sin 3\theta \begin{cases} 0 < \theta < \frac{\pi}{2} \\ \pi < \theta < \frac{3\pi}{2} \end{cases} \\ F_2(\theta) \cos\theta + G_2(\theta) \sin\theta + F_4(\theta) \cos 3\theta + G_4(\theta) \sin 3\theta \begin{cases} \frac{\pi}{2} < \theta < \pi \\ \frac{3\pi}{2} < \theta < 2\pi \end{cases} \end{cases} \tag{53}$$

where $\theta = \omega t - kx$,

$$F_1 = \frac{8\, A_1(x) b^2\, \Lambda L_c^2\, 3!}{\pi^4 C} \left[1 + \frac{\gamma^3}{3!} \frac{\tau}{A_1(x)} e^{-\frac{\tau}{A_1(x)}}\right] \tag{54}$$

$$G_1 = \frac{8\, A_1(x) b^2\, \Lambda L_c^4\, 5!}{\pi^4 C} \cdot \frac{\omega d}{\beta^2} \left[1 + \frac{\gamma^5}{5!} \frac{\tau}{A_1(x)} e^{-\frac{\tau}{A_1(x)}}\right] \tag{55}$$

$$F_2(\theta) = \frac{8\, A_1(x) b^2\, \Lambda L_c^2\, 3!}{\pi^4 C} \left[1 + \frac{\gamma^3}{3!} \frac{\tau}{A_1|\cos\theta|} e^{-\frac{\tau}{A_1|\cos\theta|}}\right] \tag{56}$$

$$G_2(\theta) = \frac{8\, A_1(x) b^2\, \Lambda L_c^4\, 5!}{\pi^4 C} \cdot \frac{\omega d}{\beta^2} \left[1 + \frac{5}{5!} \frac{\tau}{A_1|\cos\theta|} e^{-\frac{\tau}{A_1|\cos\theta|}}\right] \tag{57}$$

$$F_3 = \frac{8\, A_3(x) b^2\, \Lambda L_c^2\, 3!}{\pi^4 C} \left[1 + \frac{\gamma^3}{3!} \frac{\tau}{A_1(x)} e^{-\frac{\tau}{A_1(x)}}\right] \cos 3\delta_3 - \frac{8\, A_3(x) b^2\, \Lambda L_c^4\, 5!}{\pi^4 C} \cdot \frac{3\omega d}{\beta^2} \left[1 + \frac{\gamma^5}{5!} \cdot \frac{\tau}{A_1(x)} e^{-\frac{\tau}{A_1(x)}}\right] \sin 3\delta_3 \tag{58}$$

$$G_3 = \frac{8\, A_3(x) b^2\, \Lambda L_c^2\, 3!}{\pi^4 C} \left[1 + \frac{\gamma^3}{3!} \cdot \frac{\tau}{A_1(x)} \cdot e^{-\frac{\tau}{A_1(x)}}\right] \sin 3\delta_3 + \frac{8\, A_3(x) b^2\, \Lambda L_c^4\, 5!}{\pi^4 C} \cdot \frac{3\omega d}{\beta^2} \left[1 + \frac{\gamma^5}{5!} \cdot \frac{\tau}{A_1(x)} \cdot e^{-\frac{\tau}{A_1(x)}}\right] \cos 3\delta_3 \tag{59}$$

$$F_4(\theta) = \frac{8\, A_3(x) b^2\, \Lambda L_c^2\, 3!}{\pi^4 C} \left[1 + \frac{\gamma^3}{3!} \cdot \frac{\tau}{A_1|\cos\theta|} \cdot e^{-\frac{\tau}{A_1|\cos\theta|}}\right] \cos 3\delta_3 - \frac{8\, A_3(x) b^2\, \Lambda L_c^4\, 5!}{\pi^4 C} \cdot \frac{3\omega d}{\beta^2} \left[1 + \frac{\gamma^5}{5!} \cdot \frac{\tau}{A_1|\cos\theta|} \cdot e^{-\frac{\tau}{A_1|\cos\theta|}}\right] \sin 3\delta_3 \tag{60}$$

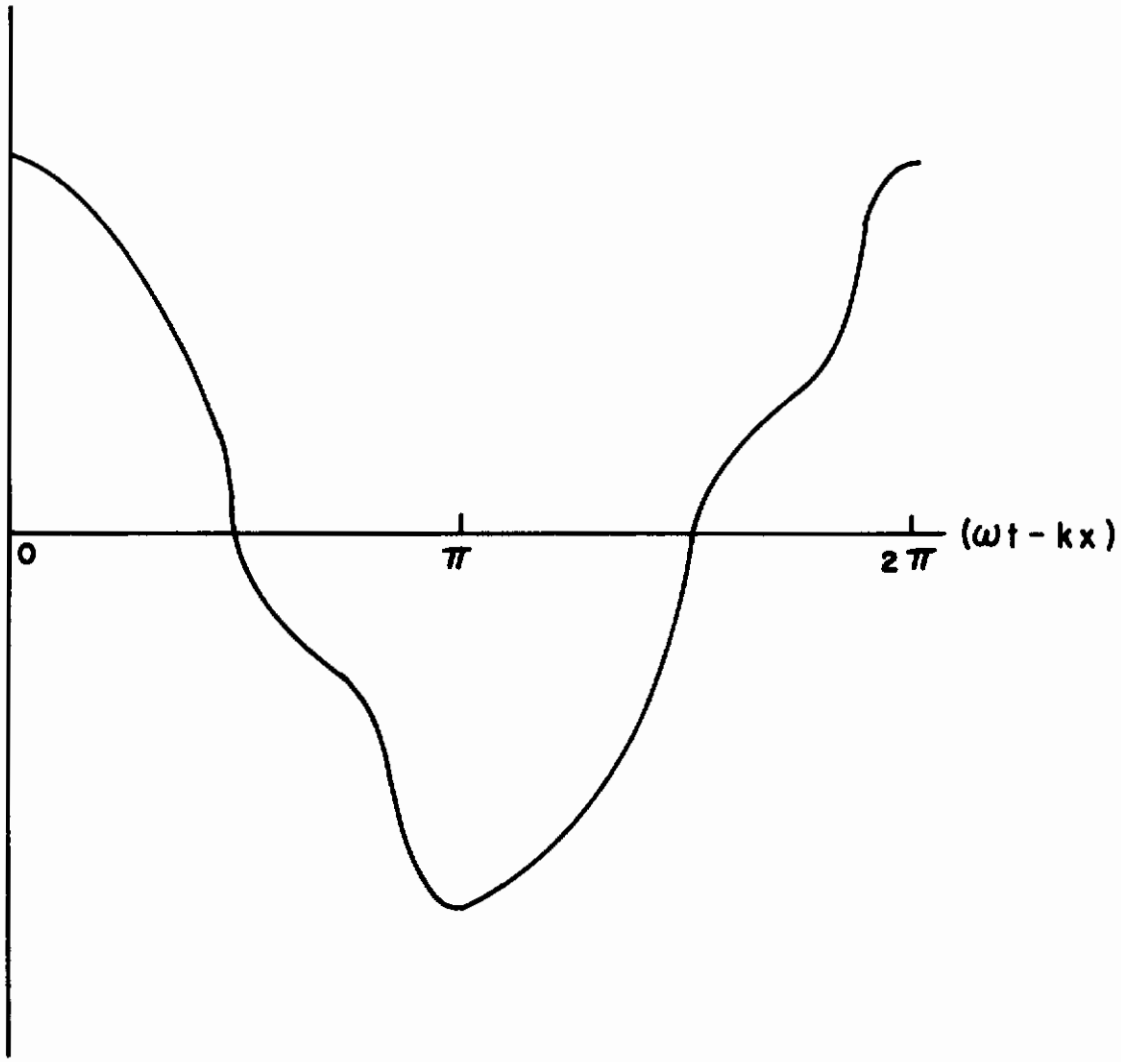

Figure 7a. The Variation of $\frac{\partial U_d}{\partial x}$ for the Cosine Term over the Course of a Cycle (schematic).

$$G_4(\theta) = \frac{8\, A_3(x) b^2\, \Lambda L_c^2\, 3!}{\pi^4 C}\left[1 + \frac{\gamma^3}{3!}\cdot\frac{\tau}{A_1|\cos\theta|}\cdot e^{-\frac{\tau}{A_1|\cos\theta|}}\right]\sin 3\delta_3$$

$$+ \frac{8\, A_3(x) b^2\, \Lambda L_c^4\, 5!}{\pi^4 C}\cdot\frac{3\omega d}{\beta^2}\left[1 + \frac{\gamma^5}{5!}\cdot\frac{\tau}{A_1|\cos\theta|}\cdot e^{-\frac{\tau}{A_1|\cos\theta|}}\right]\cos 3\delta_3 \qquad (61)$$

Now, $(\frac{\partial u_d}{\partial x})$ given in Equation (53) can be expanded into Fourier series where the fundamental and third harmonic terms are retained. The second harmonic terms vanish because of symmetry.

$$\frac{\partial u_d}{\partial x} = a_1 \cos\theta + b_1 \sin\theta + a_3 \cos 3\theta + b_3 \sin 3\theta\ , \qquad (62)$$

where

$$a_1 = \frac{1}{\pi}\left[\int_0^{\frac{\pi}{2}} (F_1 \cos\lambda + G_1 \sin\lambda)\cos\lambda\, d\lambda + \int_{\frac{\pi}{2}}^{\pi} (F_2(\lambda)\cos\lambda + G_2(\lambda)\sin\lambda)\cos\lambda\, d\lambda\right.$$

$$\left. + \int_{\pi}^{\frac{3}{2}\pi} (F_1 \cos\lambda + G_1 \sin\lambda)\cos\lambda\, d\lambda + \int_{\frac{3}{2}\pi}^{2\pi} (F_2(\lambda)\cos\lambda + G_2(\lambda)\sin\lambda)\cos\lambda\, d\lambda\right]$$

$$b_1 = \frac{1}{\pi}\left[\int_0^{\frac{\pi}{2}} (F_1 \cos\lambda + G_1 \sin\lambda)\sin\lambda\, d\lambda + \int_{\frac{\pi}{2}}^{\pi} (F_2(\lambda)\cos\lambda + G_2(\lambda)\sin\lambda)\sin\lambda\, d\lambda\right.$$

$$\left. + \int_{\pi}^{\frac{3}{2}\pi} (F_1 \cos\lambda + G_1 \sin\lambda)\sin\lambda\, d\lambda + \int_{\frac{3}{2}\pi}^{2\pi} (F_2(\lambda)\cos\lambda + G_2(\lambda)\sin\lambda)\sin\lambda\, d\lambda\right]\ ,$$

$$a_3 = \frac{1}{\pi}\left[\int_0^{\frac{\pi}{2}} (F_1 \cos\lambda + G_1 \sin\lambda + F_3 \cos 3\lambda + G_3 \sin 3\lambda) \cos 3\lambda \, d\lambda \right.$$

$$+ \int_{\frac{\pi}{2}}^{\pi} (F_2(\lambda) \cos\lambda + G_2(\lambda) \sin\lambda + F_4(\lambda) \cos 3\lambda + G_4(\lambda) \sin 3\lambda) \cos 3\lambda \, d\lambda$$

$$+ \int_{\pi}^{\frac{3}{2}\pi} (F_1 \cos\lambda + G_1 \sin\lambda + F_3 \cos 3\lambda + G_3 \sin 3\lambda) \cos 3\lambda \, d\lambda$$

$$\left. + \int_{\frac{3}{2}\pi}^{2\pi} (F_2(\lambda) \cos\lambda + G_2(\lambda) \sin\lambda + F_4(\lambda) \cos 3\lambda + G_4(\lambda) \sin 3\lambda) \cos 3\lambda \, d\lambda \right] ,$$

$$b_3 = \frac{1}{\pi}\left[\int_0^{\frac{\pi}{2}} (F_1 \cos\lambda + G_1 \sin\lambda + F_3 \cos 3\lambda + G_3 \sin 3\lambda) \sin 3\lambda \, d\lambda \right.$$

$$+ \int_{\frac{\pi}{2}}^{\pi} (F_2(\lambda) \cos\lambda + G_2(\lambda) \sin\lambda + F_4(\lambda) \cos 3\lambda + G_4(\lambda) \sin 3\lambda) \sin 3\lambda \, d\lambda$$

$$+ \int_{\pi}^{\frac{3}{2}\pi} (F_1 \cos\lambda + G_1 \sin\lambda + F_3 \cos 3\lambda + G_3 \sin 3\lambda) \sin 3\lambda \, d\lambda$$

$$\left. + \int_{\frac{3}{2}\pi}^{2\pi} (F_2(\lambda) \cos\lambda + G_2(\lambda) \sin\lambda + F_4(\lambda) \cos 3\lambda + G_4(\lambda) \sin 3\lambda) \sin 3\lambda \, d\lambda \right] .$$

Since it appears to be impossible to carry out the above integrals analytically, one has to evaluate the coefficients a_1, b_1, a_3, and b_3 either by making suitable approximations or by computing numerically.

The nonlinear factor $D = \frac{\tau}{A_1} e^{-\frac{\tau}{A_1}}$ is plotted against $\frac{A_1}{\tau}$ in Figure 7b. The factor D has a maximum when $\frac{A_1}{\tau} = 1$, or $A_1 = \tau$. Since the stress amplitude A_1 in the case of interest to us can be assumed to be much smaller than τ, it is sufficient to consider only the region where $0 \leq \frac{A_1}{\tau} << 1$. If the factor D is approximated by a polynomial in $\frac{A_1}{\tau}$, the polynomial should contain only the terms in even powers, because of the symmetry requirement, and there should be no constant term because

$$\left[\frac{\tau}{A_1} e^{-\frac{\tau}{A_1}}\right]_{A_1=0} = 0.$$

Thus, the lowest term of the polynomial is $p(\frac{A_1}{\tau})^2$, where p is a constant. If one replaces the nonlinear factor D with the first term of the polynomial, $p(\frac{A_1}{\tau})^2$ as a first approximation, the following results:

$$a_1 = \frac{8b^2\Lambda L_c^2 3!}{\pi^4 C} \cdot A_1 + \frac{7b^2\Lambda L_c^2\gamma^3 p}{\pi^4 C\ \tau^2} \cdot (1 - \frac{4L_c^2\gamma^2}{7\pi} \cdot \frac{\omega d}{\beta^2}) \cdot A_1^3 \tag{63}$$

$$b_1 = \frac{8b^2\Lambda L_c^4 5!}{\pi^4 C} \cdot \frac{\omega d}{\beta^2} \cdot A_1 + \frac{b^2\Lambda L_c^2\gamma^3 p}{\pi^4 C\ \tau^2} \cdot (5L_c^2\gamma^2 \frac{\omega d}{\beta^2} - \frac{4}{\pi}) \cdot A_1^3 \tag{64}$$

$$a_3 = \frac{b^2\Lambda L_c^2\gamma^3 p}{\pi^4 C\ \tau^2} \cdot (1 - \frac{20}{3\pi} \cdot L_c^2\gamma^2 \cdot \frac{\omega d}{\beta^2})\ A_1^3 \tag{65}$$

$$+ \frac{8b^2\Lambda L_c^2 3!}{\pi^4 C} (\cos 3\delta_3 - 20L_c^2 \cdot \frac{3\omega d}{\beta^2} \cdot \sin 3\delta_3) \cdot A_3$$

$$b_3 = \frac{b^2\Lambda L_c^2\gamma^3 p}{\pi^4 C\ \tau^2} (\frac{4}{3\pi} + L_c^2\gamma^2 \cdot \frac{\omega d}{\beta^2}) \cdot A_1^3 \tag{66}$$

$$+ \frac{8b^2\Lambda L_c^2 3!}{\pi^4 C} (\sin 3\delta_3 + 20L_c^2 \cdot \frac{3\omega d}{\beta^2} \cdot \cos 3\delta_3) \cdot A_3$$

Inserting Equations (48), (52) and (62) along with relations (63), (64), (65) and (66) into Equation (2), one obtains the following relations, from which one can determine the amplitudes A_1 and A_3 to this approximation:

$$\frac{\partial^2 A_1}{\partial x^2} - k^2 A_1 = -\rho\omega^2(a_1 + \frac{A_1}{E_1}) \tag{67}$$

$$2k \frac{\partial A_1}{\partial x} = -\rho\omega^2 b_1 \tag{68}$$

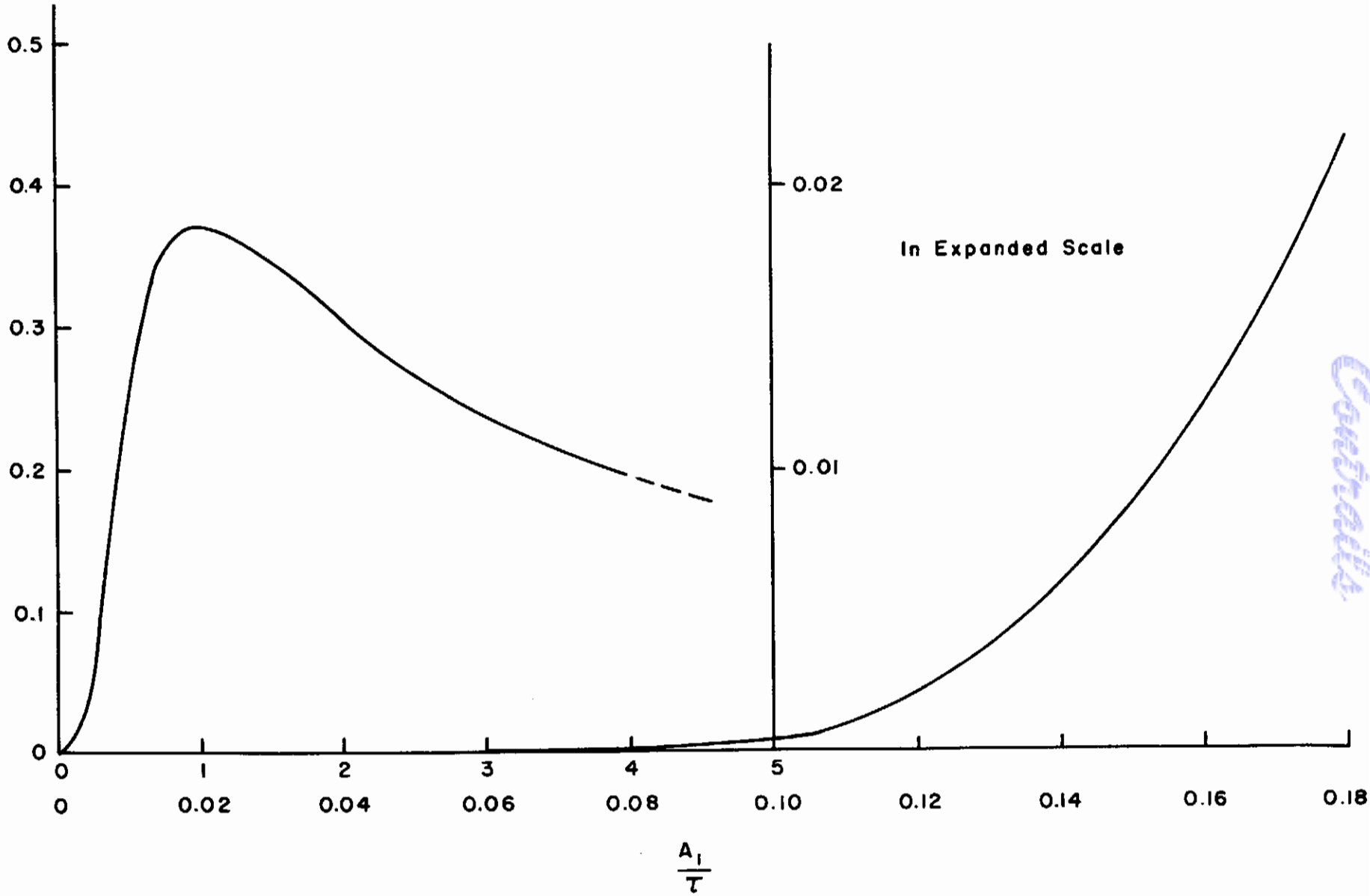

Figure 7 b. Factor $\frac{\tau}{A_1} e^{-\frac{\tau}{A_1}}$ as a function of $\frac{A_1}{\tau}$.

$$\left(\frac{\partial^2 A_3}{\partial x^2} - 9k^2 A_3\right) \cos 3\delta_3 - 6k \frac{\partial A_3}{\partial x} \sin 3\delta_3 = -9\rho\omega^2 \left(a_3 + \frac{A_3}{E_1} \cos 3\delta_3\right) \tag{69}$$

$$\left(\frac{\partial^2 A_3}{\partial x^2} - 9k^2 A_3\right) \sin 3\delta_3 + 6k \frac{\partial A_3}{\partial x} \cos 3\delta_3 = -9\rho\omega^2 \left(b_3 + \frac{A_3}{E_1} \sin 3\delta_3\right) \tag{70}$$

From Equations (67) and (68), one obtains

$$A_1 = A_{10}\, e^{-\alpha_1 x}, \tag{71}$$

where

$$\alpha_1 = \frac{\rho\omega^2}{2k} \left[\frac{8b^2 \Lambda L_c^4 5!}{\pi^4 C} \cdot \frac{\omega d}{\beta^2} + \frac{b^2 \Lambda L_c^2 \gamma^3 p}{\pi^4 C} \cdot \left(\frac{A_1}{\tau}\right)^2 \cdot \left(5 L_c^2 \gamma^2 \frac{\omega d}{\beta^2} - \frac{4}{\pi}\right)\right], \tag{72}$$

and A_{10} is the amplitude of the fundamental wave at x = 0;

and

$$k^2 = \frac{\rho\omega^2}{E_1} \left[1 + \frac{8b^2 \Lambda L_c^2 3!}{\pi^4 C} + \frac{7b^2 \Lambda L_c^2 \gamma^3 p}{\pi^4 C} \cdot \left(\frac{A_1}{\tau}\right)^2 \cdot \left(1 - \frac{4}{7\pi} L_c^2 \gamma^2 \frac{\omega d}{\beta^2}\right)\right]. \tag{73}$$

From Equations (69) and (70),

$$A_3 = \frac{3}{2} \frac{\rho\omega^2}{k} \frac{b^2 \Lambda L_c^2 \gamma^3 p}{\pi^4 C \tau^2} \left\{\left(1 - \frac{20}{2\pi} L_c^2 \gamma^2 \frac{\omega d}{\beta^2}\right) \sin 3\delta_3 - \left(\frac{4}{3\pi} + L_c^2 \gamma^2 \frac{\omega d}{\beta^2}\right) \cos 3\delta_3\right\} A_{10}^3 \cdot \frac{e^{-3\alpha_1 x} - e^{-\alpha_3 x}}{\alpha_3 - 3\alpha_1} \tag{74}$$

where

$$\alpha_3 = \frac{3}{2} \frac{\rho\omega^2}{k} \cdot \frac{8b^2 \Lambda L_c^4 5!}{\pi^4 C} \cdot \frac{3\omega d}{\beta^2} \tag{75}$$

and

$$\tan 3\delta_3 = \frac{6k\left(1 - \frac{20}{2\pi} L_c^2\gamma^2 \frac{\omega d}{\beta^2}\right) + (\alpha_3 + 3\alpha_1)\left(\frac{4}{3\pi} + L_c^2\gamma^2 \frac{\omega d}{\beta^2}\right)}{(\alpha_3 + 3\alpha_1)\left(1 - \frac{20}{2\pi} L_c^2\gamma^2 \frac{\omega d}{\beta^2}\right) - 6k\left(\frac{4}{3\pi} + L_c^2\gamma^2 \frac{\omega d}{\beta^2}\right)} \qquad (76)$$

IV. Experimental Results and Discussion

The expression for the amplitude of the third harmonic (expression (41)) may be rewritten in the following way:

$$A_3 = K \cdot N \cdot A_{10}^3 \cdot f_1(L) \cdot f_2(\alpha, x) \tag{77}$$

where

$$K = \frac{12\rho\omega^2 b^4 \Omega R^3 CC'}{k A^4}$$

$f_1(L)$: loop length factor $= \dfrac{1}{S_o^{3/2} T_o^{1/2} L_o^4}$

$f_2(\alpha, x)$: attenuation factor $= \dfrac{e^{-3\alpha_1 x} - e^{-\alpha_3 x}}{\alpha_3 - 3\alpha_1}$

The experimental scheme to test the validity of the expression (77) is, then, to vary each factor appearing in the expression and observe the corresponding change in A_3.

The factor N (dislocation density) may be varied by deforming the sample plastically.

The factor A_{10} (amplitude of the fundamental wave) can be varied by simply inserting an attenuator in the driving circuit.

The factor $f_1(L)$ may be varied in two ways: 1) by investigating specimens of different impurity content, because the effective loop length of an annealed crystal is primarily determined by the impurity content. 2) by applying a small static bias stress to the specimen. The bias stress should be small enough so that no multiplication of dislocations takes place. With this procedure, some of the dislocations in the crystal will break away from the pinning points, resulting in an increase in the average loop length, without changing the dislocation density.

The factor $f_2(\alpha, x)$ may be tested by observing the echo pattern of the third harmonic resulting from the multiple reflections.

In the following, the experimental results obtained along the scheme outlined above are presented.

Experimental Technique

The general technique for the detection and measurement of ultrasonic harmonics was discussed in Ref. 1 and 3, and will not be repeated here.

Aluminum single crystals have been prepared with resistivity ratios varying over a wide range. Zone refined aluminum of several degrees of purity was used in a modified Bridgman technique to grow specimens whose long axes lie along several directions of high symmetry. The resistivity ratio was measured using the eddy current technique described by Bean, et. al.[15]. The size of all the specimens was 0.96 × 0.96 × 12.7 cm. Details of deforming the specimens in an Instron testing machine are described elsewhere[16]; the application of the static bias stress is achieved by hanging small weights on a grip attached to the lower end of the specimen, as shown in Figure 8.

Also indicated in Figure 8 are the details of the experimental arrangement, in which a 10 mc longitudinal pulsed signal is introduced into one end of the specimen by means of an appropriate quartz transducer. The 30 mc output is obtained at the opposite end of the specimen with another transducer. With this arrangement it is possible to measure simultaneously the amplitude of the third harmonic and the attenuation of the fundamental wave.

Effect of Loop Length: Impurity Content and Bias Stress

As shown in section II, it is expected that the dislocations with smaller C values (edge dislocations) will generate larger harmonics, if other factors are identical. With this expectation, the amplitude of the third harmonic due to edge dislocations and the corresponding attenuation shown in Figure 5 are replotted in logarithmic scale as a function of loop length in Figure 9. It is seen that the third harmonic amplitude has a maximum at a loop length of $L_m \sim 2 \times 10^{-4}$cm, if one uses the numerical values quoted in section II for the factors A, B, C and ω. As mentioned above, the effective loop length of an annealed specimen is determined primarily by impurity content, and a small bias stress makes the loop length increase. Thus, if the loop length in the sample before the application of a bias stress (initial loop length) lies somewhat below L_m, for example having a value given by the point A indicated in Figure 9 (which may correspond to the loop length in a relatively impure specimen), then the amplitude of the third harmonic will increase initially with the bias stress. If the initial loop length in the sample is less than but close to L_m (point B for example in Figure 9), which may correspond to the loop length in a specimen of intermediate purity, the amplitude of the third harmonic will go through a maximum as the bias stress increases. Finally, if the initial loop length is larger than L_m, point C for example (which may correspond to the loop length in a specimen of highest purity used in these experiments), the amplitude of the third harmonic will simply decrease with the bias stress.

The experimental results are shown in Figure 10. Here, three samples of resistivity ratios 3100, 750 and 300 (⟨100⟩ axial orientation) are subjected to a bias stress ranging from zero to 1.25×10^6 dynes/cm^2. The resulting change in the amplitude of the third harmonic is plotted in db scale, and the values at zero bias stress are normalized for each sample to the initial amplitude. It is

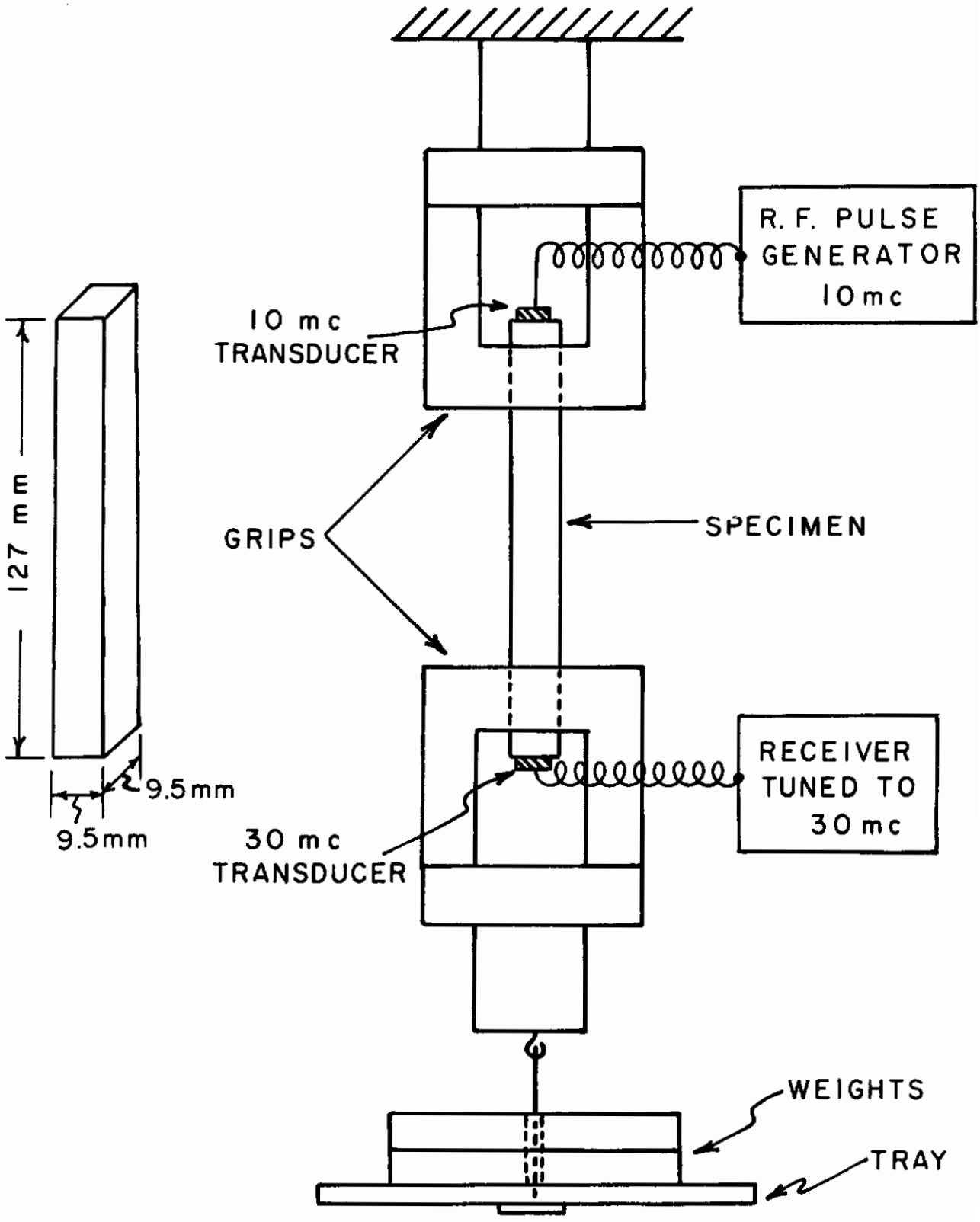

FIGURE 8.
EXPERIMENTAL EQUIPMENT (SCHEMATIC)

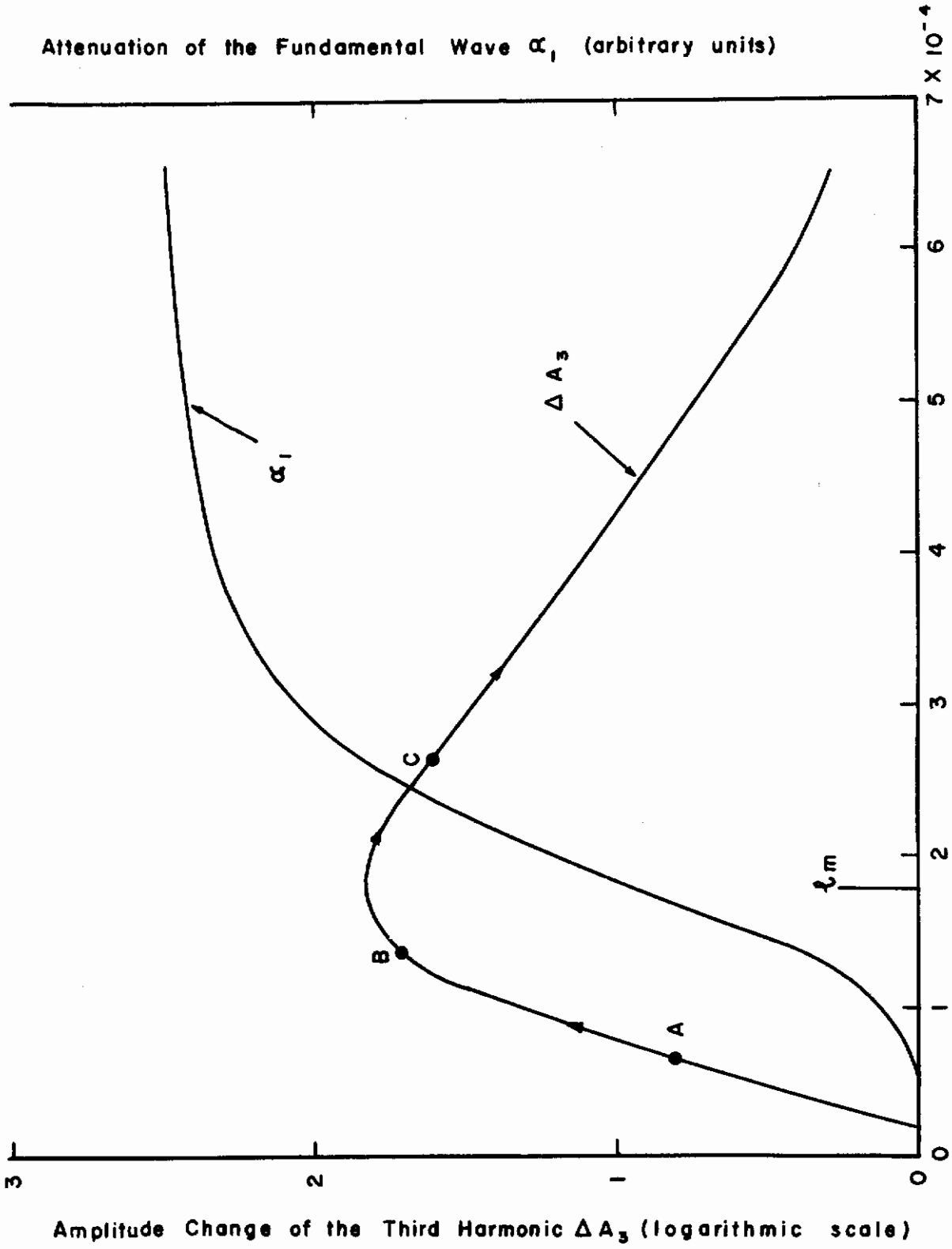

Figure 9.

readily seen that the behavior of the third harmonic amplitude follows the above prediction; i.e., in the impure specimen (R = 300) the amplitude of the third harmonic simply increases with bias stress, in the intermediate specimen (R = 750) the amplitude goes through a maximum, and in the zone refined specimen (R = 3100) the amplitude simply decreases with increasing bias stress.

In each of the above mentioned tests, the attenuation of the fundamental wave as a function of bias stress was also measured, and the results are shown in Figure 10. It appears that for samples in the annealed state, the amplitude of the third harmonic is a much more sensitive guide to the changes in dislocation loop length that occur under the influence of applied bias stress than is the attenuation.

Effect of Plastic Deformation

For the purpose of studying the influence of changes in dislocation density and distribution, it is of interest to observe the effect of plastic deformation on the amplitude of the third harmonic in samples of different purity. In Figure 11 the results of experiments on the sample with a ⟨100⟩ axial orientation and a resistivity ratio of 300 are shown. The amplitude of the third harmonic and the attenuation of the fundamental wave are shown as a function of an applied tensile bias stress that ranges from 0 to 4.0×10^6 dynes/cm^2. In the annealed state, A_3 increases with increasing tensile bias stress, while α_1 changes by less than 0.01 db/μsec. After deforming the specimen in tension to 6.7×10^7 dynes/cm^2 the same amount of bias stress as used in the annealed state was applied again. (After deformation, however, a certain amount of time was allowed to elapse before the experiment was performed again. Usually we waited until A_3 and α_1 did not change measurably in a time equal to the time it takes to perform the experiment. In most cases this was about 2 hours). The amplitude of the third harmonic now goes through a maximum and the attenuation change has increased to 0.06 db/μsec.

Again it is possible to make a comparison with the theoretical curve. Following the analysis applied previously, it appears that in the annealed state the average loop length may correspond to a point close to A in Figure 9. On the other hand, in the deformed state the average loop length appears to be longer, corresponding perhaps to a point close to B, since the amplitude of the third harmonic goes through a maximum as a function of bias stress.

Changes in the effect of bias stress on A_3 and α_1 due to plastic deformation were also observed in a ⟨111⟩ sample of resistivity ratio 1200, and in the ⟨100⟩ samples of resistivity ratio 3100. In the case of the former, tests were performed with the specimen in the annealed state as well as after the application of a tensile stress of 3.2×10^7 dynes/cm^2 and a tensile stress of 6.4×10^7 dynes/cm^2. Figure 12 indicates the results when the bias stress was varied from 0 to 1.0×10^6 dynes/cm^2. A_3 in the annealed state initially increases and subsequently goes through a maximum when the bias stress reaches about 0.75×10^6 dynes/cm^2. After one deformation A_3 goes through a maximum at $\sigma_o = 0.25 \times 10^6$ dynes/cm^2, and after the second deformation A_3 decreases with increasing bias stress. The change in attenuation α_1 increases from the annealed state as the amount of plastic deformation increases. Similar changes were also

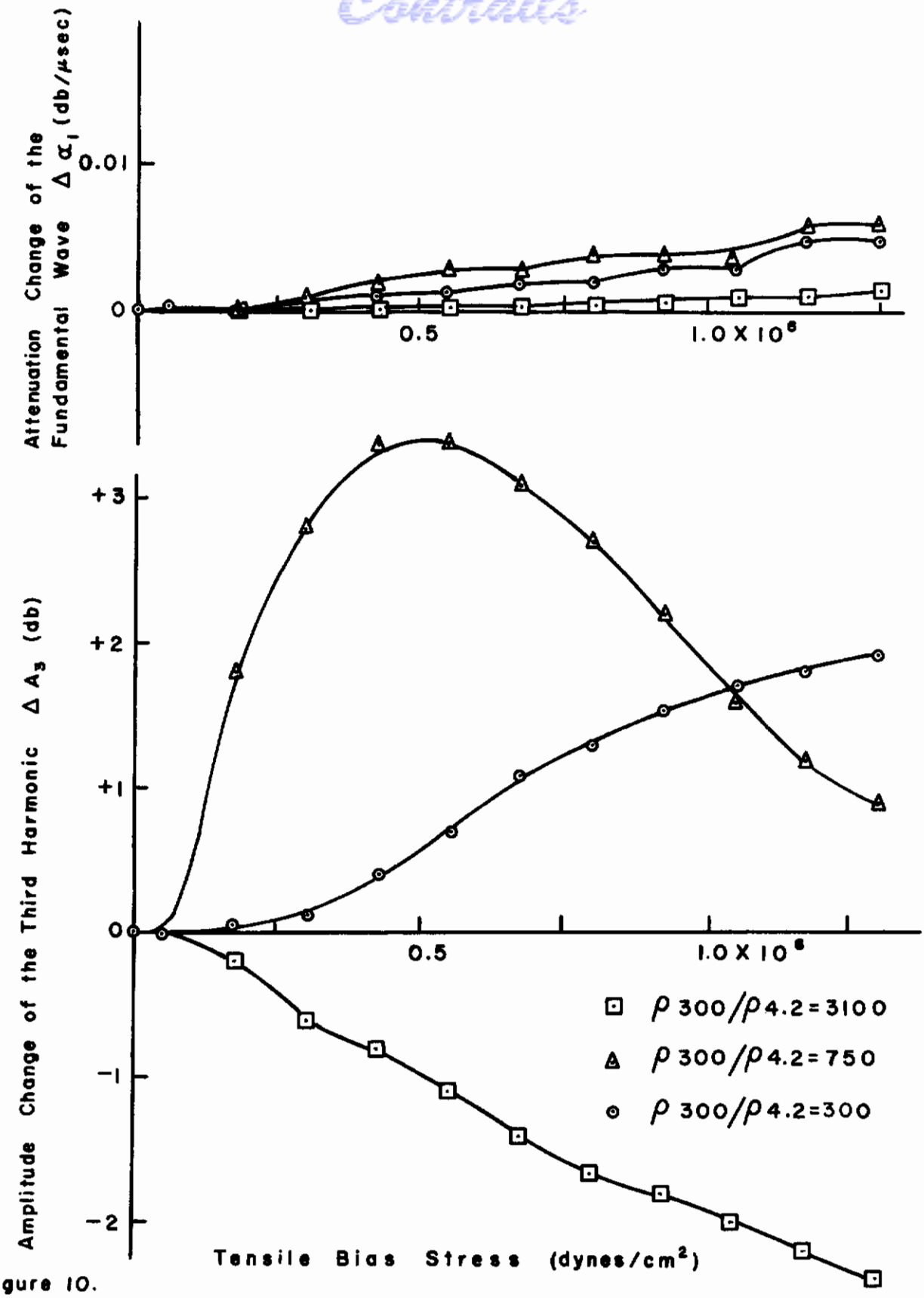

Figure 10.
Effect of Impurity Concentration on Third Harmonic in <100> Annealed Specimens.

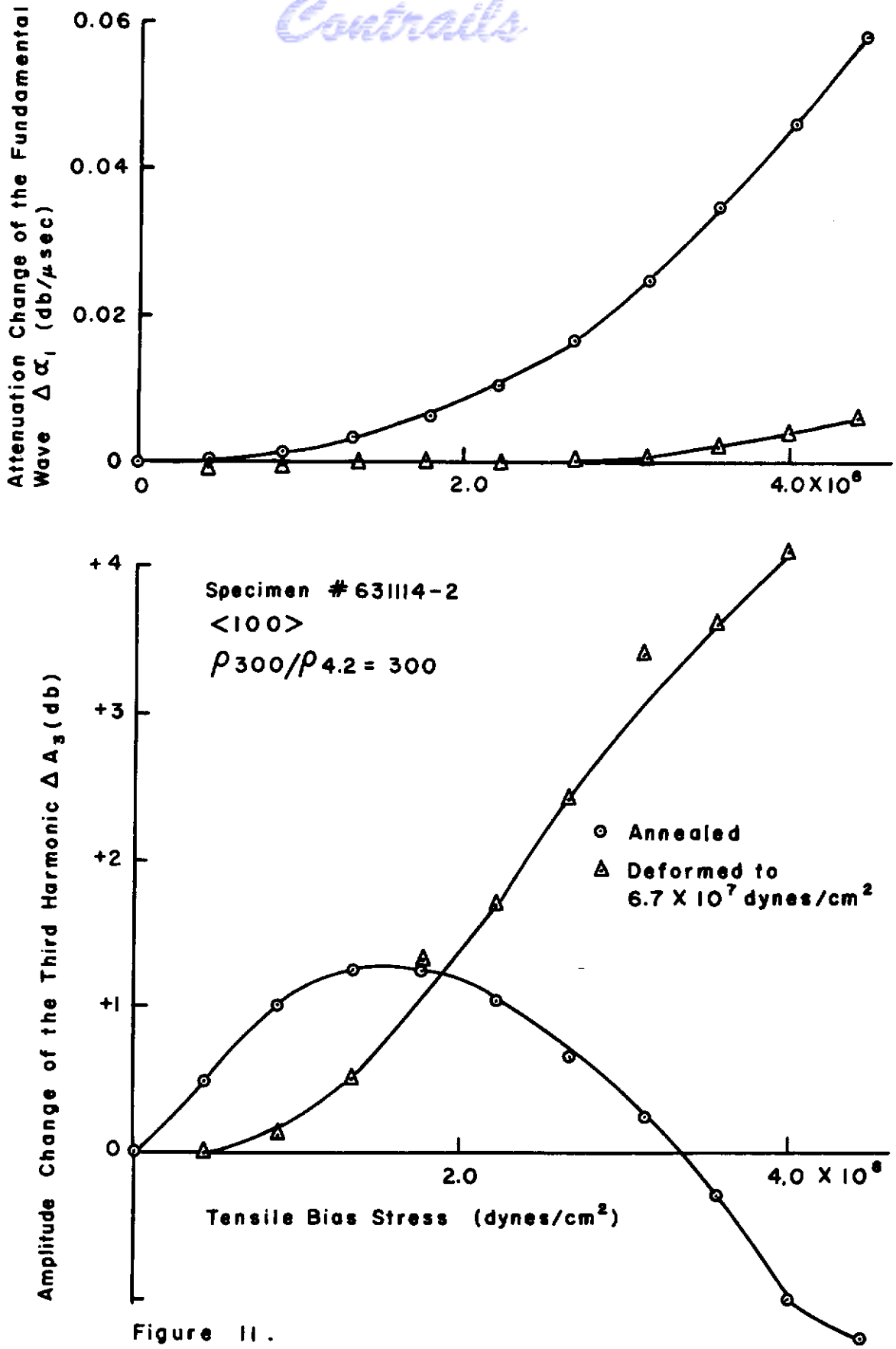

Figure 11.
Effect of Plastic Deformation on the Amplitude of the Third Harmonic.

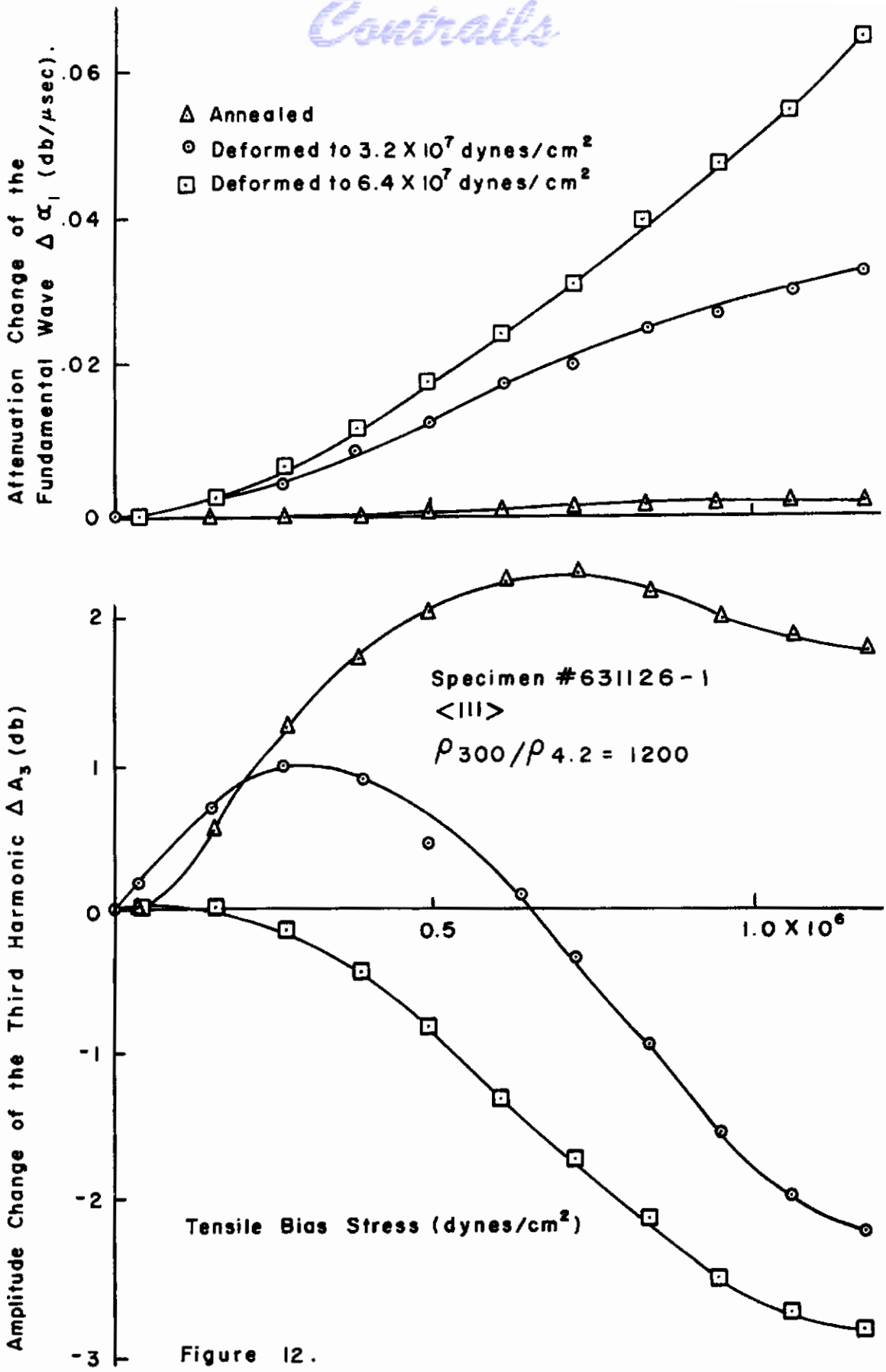

Figure 12.
Effect of Plastic Deformation on the Amplitude of the Third Harmonic and Attenuation.

observed in the sample with the ⟨100⟩ axis and resistivity ratio of 3100. After measurements were performed on this annealed specimen, it was deformed in tension to 0.9×10^7 dynes/cm^2. (see Figure 13). Once again, the effect of straining the sample beyond the yield point was to increase the sensitivity of the attenuation to the small bias stress. The third harmonic undergoes a decrease in amplitude both before and after plastic deformation.

It appears that in these specimens the process of plastic deformation increases the average loop length. In other words, as we proceed from the annealed state to the state of increased deformation, the average loop length appears to increase from points A to B to C as shown on the theoretical curve in Figure 9. This effect and the increased sensitivity of α_1 to bias stress will now be discussed separately.

One must first consider the configuration of the dislocation network in the annealed state and after plastic deformation has occurred. In a typical annealed sample there is probably a dislocation density of about 10^6 cm^{-2}. The dislocations may be expected to lie in the various slip systems and possibly in very low angle boundaries which make up mosaic or polygonal structure that may exist in the as-grown crystal. Dislocations in such grain boundaries are probably immobile and do not contribute to the ultrasonic properties at the frequencies used in these experiments. In the absence of detailed experimental knowledge on the dislocation structure, we assume that dislocations form an intersecting network whose average loop length is L. Because of migration of impurities to dislocation lines, the effective average loop length ℓ_o is shorter than L and is determined by the density of impurities in the crystal and the thermal history of the specimen.

Now, under the influence of a small amplitude oscillatory stress, the dislocation segments between impurity pinning points oscillate with a nonlinear behavior dependent on the average distance between pinning points. The application of a bias stress in the range used in our experiments causes an increase of the average loop length by breakaway, but not to the point of exceeding the network loop length L.

However, when a sample is plastically deformed, the network loop length is decreased on the average, especially in samples whose axes lie along directions of high symmetry and hence have several active slip systems in which moving dislocations can intersect. In addition, of course, there is dislocation multiplication which further tangles the network.

There are two possibilities, however, that may aid in explaining why changes in A_3 with bias stress correspond to an apparent increase in effective dislocation loop length after plastic deformation. In the first place, while the network loop length probably becomes shorter, the deformation process upsets the distribution of impurities which pin dislocation lines. Such a change in the distribution may for a time lead to a longer average distance between impurities. For example, in the deformation process the primary dislocation in a Frank-Read source, pinned heavily at network or intersection points may, for a time, be torn away from some of the intermediate impurity pinning points.

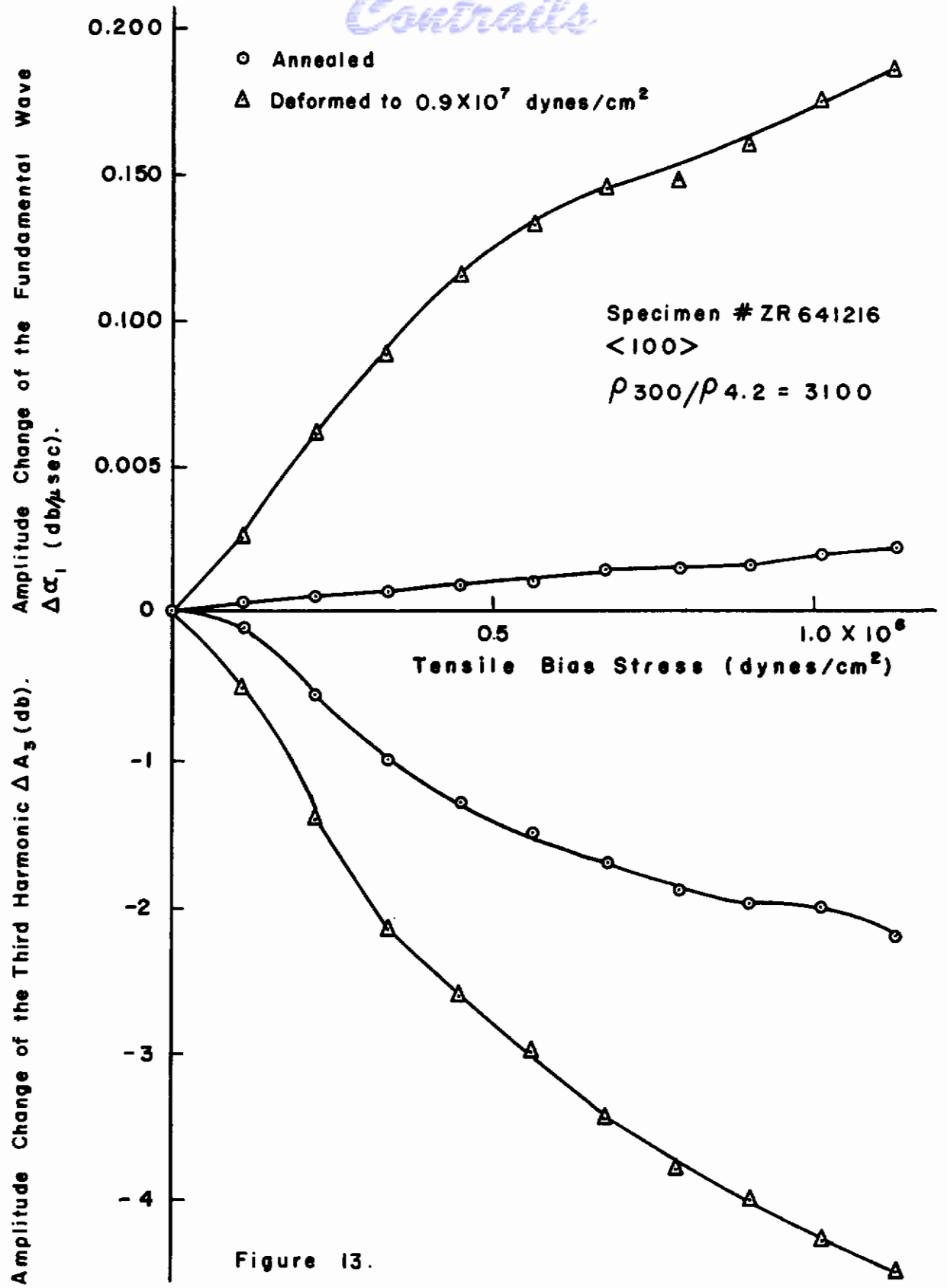

Figure 13.

Effect of Plastic Deformation on the Amplitude of the Third Harmonic.

Probably more important is the fact that the emitted loops from this source should at first be relatively free of impurity pinning and thus constitute a source of long dislocation lines. Therefore, if the third harmonic is measured as a function of bias stress about 2 hours after plastic deformation takes place, the combined effect of removal of impurity atoms from existing dislocations and the production of new unpinned dislocations create a situation in which the average effective loop length appears to be longer than in the annealed state.

The experimental fact that the amplitude of the third harmonic as a function of bias stress (when interpreted in terms of the nonlinear string model) behaves as though deformation increases the dislocation loop length suggests a further mechanism that may be operative. This relates to the idea that the application of stress greater than the macroscopic yield point of a metal can lead to regions of internal stress such as dislocation pile-ups within the specimen. This notion can best be discussed by first considering the conditions for equilibrium for a dislocation that has moved into the vicinity of an obstacle. Such conditions exist when the sum of the applied stress σ_e, and the stress due to the obstacle σ_i are equal to zero:

$$\sigma_e - \sigma_i = 0$$

This condition holds when the dislocation is a straight, or practically straight line impinging on a long continuous obstacle such as a grain boundary or similar immobile array. Now if a sequence of similar dislocations emanate from a source and move toward the obstacle, a pile-up is created with the important feature that the stress on the leading dislocation is amplified by the stress of the interacting dislocations such that the new equilibrium condition is given by $n\sigma_e = \sigma_i$, where n is the number of dislocations in the pile-up[17].

It is now obvious that the formation of such pile-ups during deformation can have the result of making an applied bias stress more effective in causing dislocations in the pile-up to break away from impurities. Therefore, after deformation, the apparent change in dislocation loop length with bias stress may appear to be larger than in the annealed state, in which the applied stress does not have the benefit of the stresses from the piled-up dislocations to aid in the breakaway process.

The same two processes that may be operating in small plastic deformation to lengthen dislocation lines, may also be responsible for the fact that the attenuation change with bias stress is greater after the specimen has been deformed than when it is annealed. 1) If, indeed, the average effective dislocation loop length is increased by plastic deformation, then one would expect a greater change in α_1 with applied bias stress following the deformation. 2) Also, the action of internal stress discussed above would make the effectiveness of bias stress in unpinning dislocations very apparent through changes in the attenuation. In addition, the greater change of the attenuation after deformation may be due in part to the fact that the dislocation density is also increased in the deformation process.

Amplitude Dependence of the Third Harmonic and of the Attenuation

It has long been thought that ultrasonic experiments in the megacycle region would not yield any dependence of the attenuation on the amplitude of the fundamental wave. However, the combination of our high power pulse generator and extremely sensitive readout units for detecting changes in the amplitude of the third harmonic and the attenuation α_1 have made it possible to observe a striking amplitude dependence in both these quantities.

Again, the experiments involve specimens in three purity ranges: R = 300, R = 1200, and R = 3100. Figures 14-19 show the attenuation α_1 and the amplitude of the third harmonic as a function of the amplitude of the fundamental wave A_1. The latter is varied usually over a range of 20db (in the case of the attenuation measurements), the maximum point in every case being the maximum power than can be introduced into the specimen without electrical discharge in the vicinity of the driving 10 mc transducer. The results of the experiments on A_3 vs A_1 are plotted in db.

For the low purity sample (R = 300), whose axial orientation is ⟨100⟩ , the attenuation change in the annealed state, shown in Figure 14, was about 0.002 db/μsec when A_1 was changed by 20 db. After deformation to 6.75×10^7 dynes/cm^2, a change of 20 db in A_1 was accompanied by a change in α_1 of 0.014 db/μsec, or about 7 times that observed when the sample was annealed. Figure 15 shows the variation of A_3 with A_1 both in the annealed state and after deformation. The behavior of the annealed specimen is such that the points fall practically on the slope 3 line, while there was slight deviation from the slope 3 condition when the measurements were made after deformation.

Similar experiments were performed on the R = 1200 sample whose long axis coincides with the ⟨111⟩ direction. On this specimen data were recorded after it was slightly handled while being put in the grips, and after deformation to 1.5×10^7 dynes/cm^2 and to 2.2×10^7 dynes/cm^2. The change in attenuation (shown in Figure 16) as a function of A_1 becomes successively larger after each of these stages, finally changing by 0.1 db/μsec after the last deformation. The amplitude of the third harmonic (see Figure 17) deviates slightly from slope 3 after annealing, and continues to deviate more with handling and with deformation.

The same general behavior (see Figures 18 and 19) is also observed in the ⟨100⟩ pure sample with R = 3100: a striking change in α_1 after the sample is deformed to 0.9×10^7 dynes/cm^2 is observed when A_1 is increased by 20 db. Likewise, with the amplitude of the third harmonic there is some deviation from slope 3 in the annealed state, and drastic deviation after deformation. To understand the nature of these amplitude dependent effects we must investigate possible mechanisms of damping and try to determine in what way they are related to the amplitude of the fundamental wave.

The situation will be first considered in which the dislocation line length is assumed not to change (except for bowing out) with changes in the amplitude A_1. In this case we are concerned with any loss that may arise due to the non-linear response of the dislocation to applied oscillatory stress. Expressions

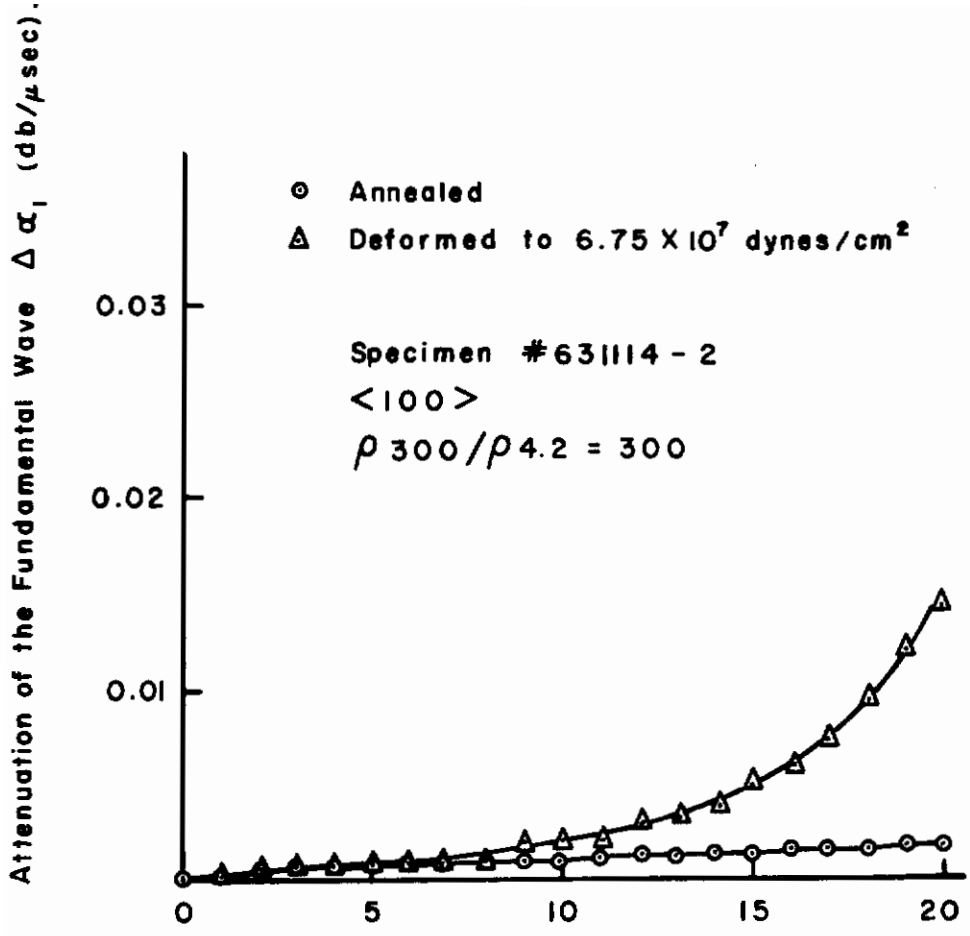

Figure 14. Amplitude of the Fundamental Wave A_1 (db). Effect of the Fundamental Wave Amplitude on the Attenuation α_1.

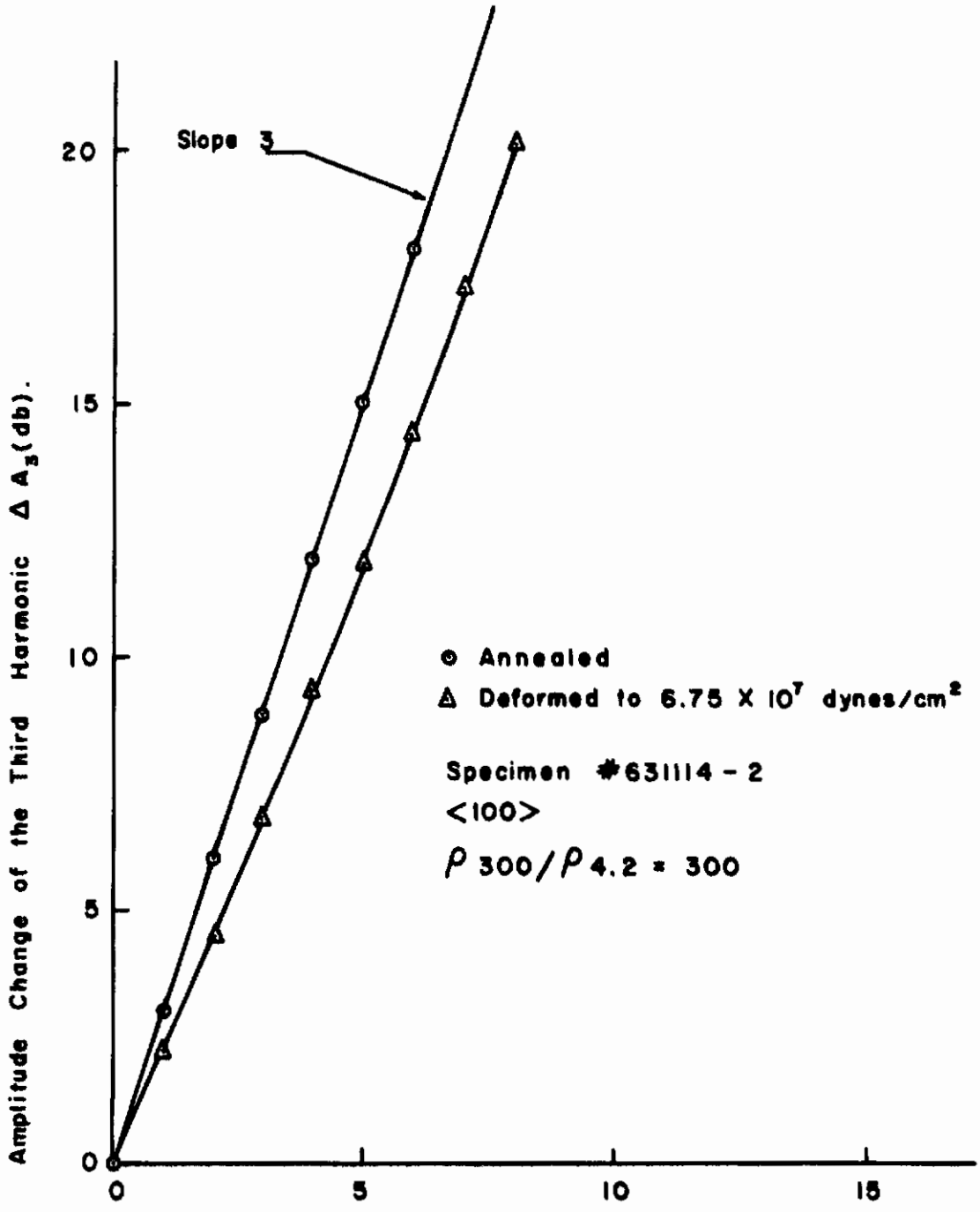

Figure 15.

Amplitude of the Fundamental Wave ΔA_1 (db).
Effect of Plastic Deformation on the Amplitude of the Third Harmonic A_3.

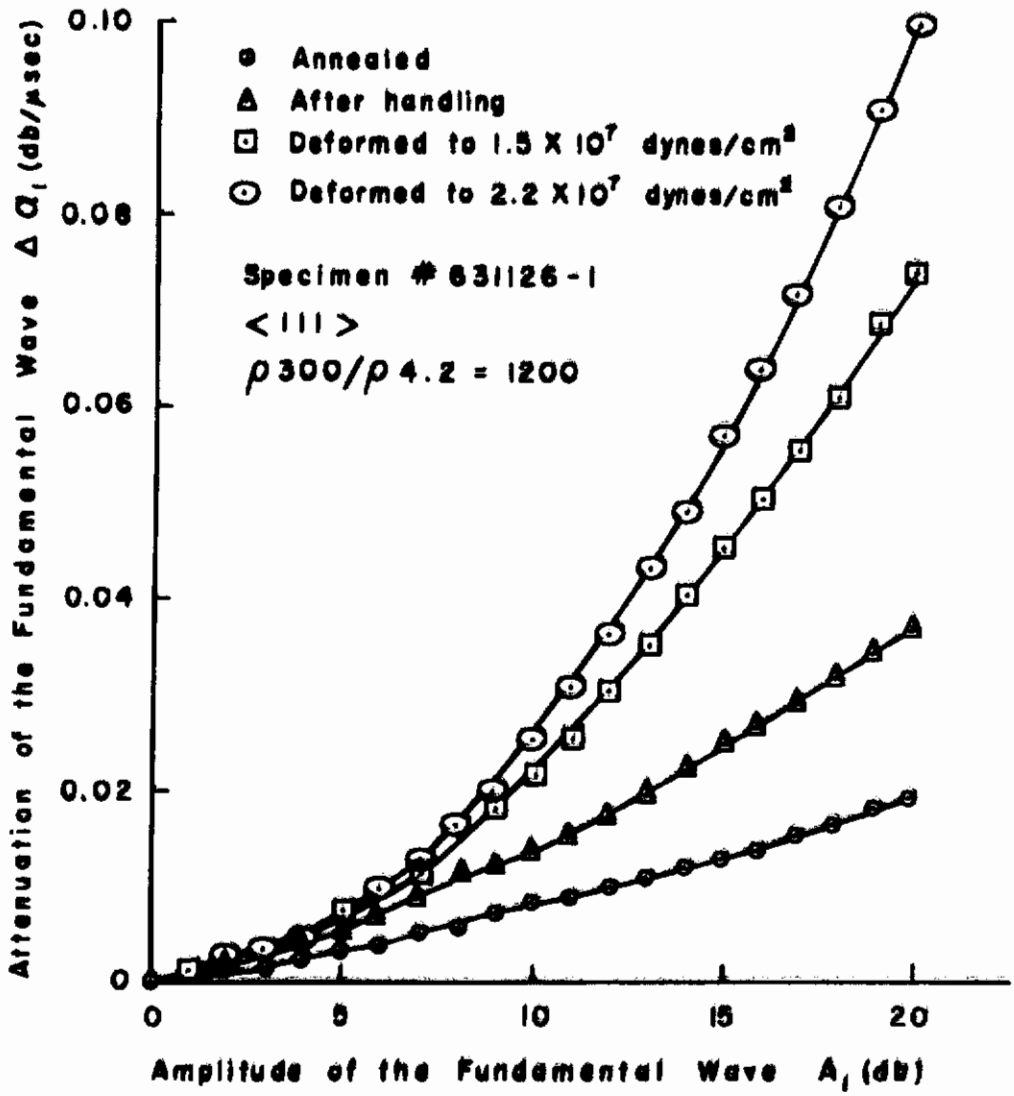

Figure 16. Effect of the Fundamental Wave Amplitude on the Attenuation α_1

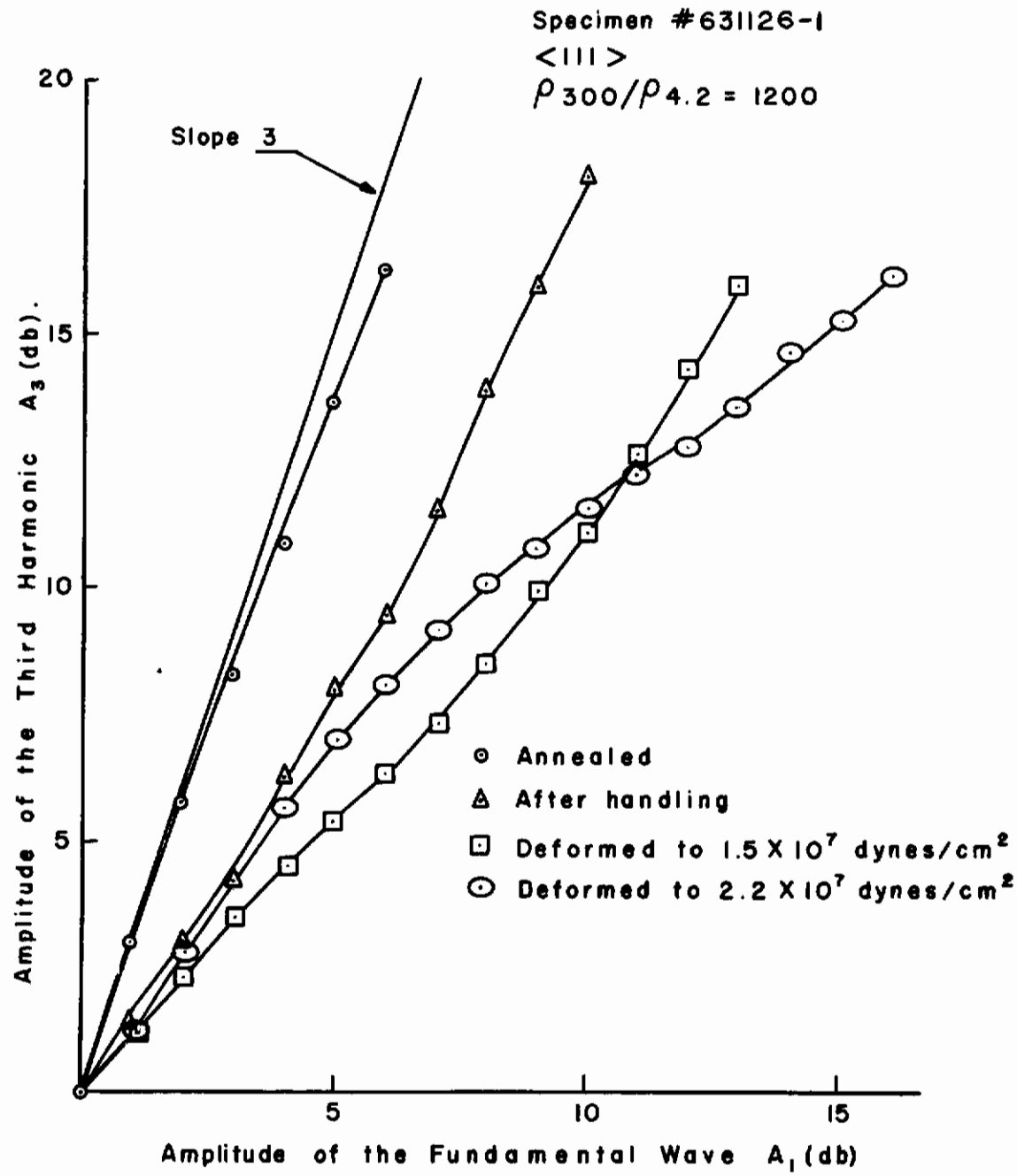

Figure 17. Effect of Plastic Deformation on the Amplitude of the Third Harmonic A_3.

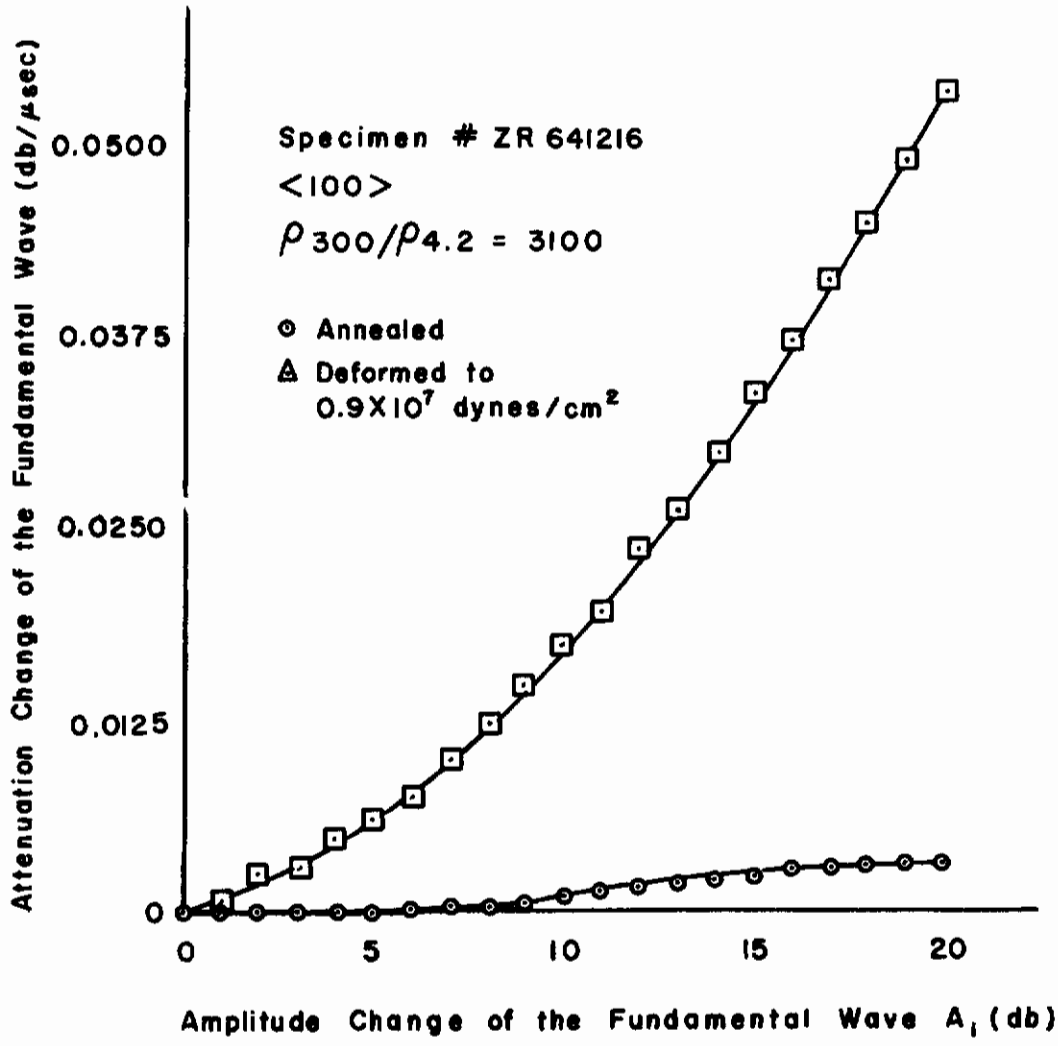

Figure 18. Effect of the Fundamental Wave Amplitude on the Attenuation α_1.

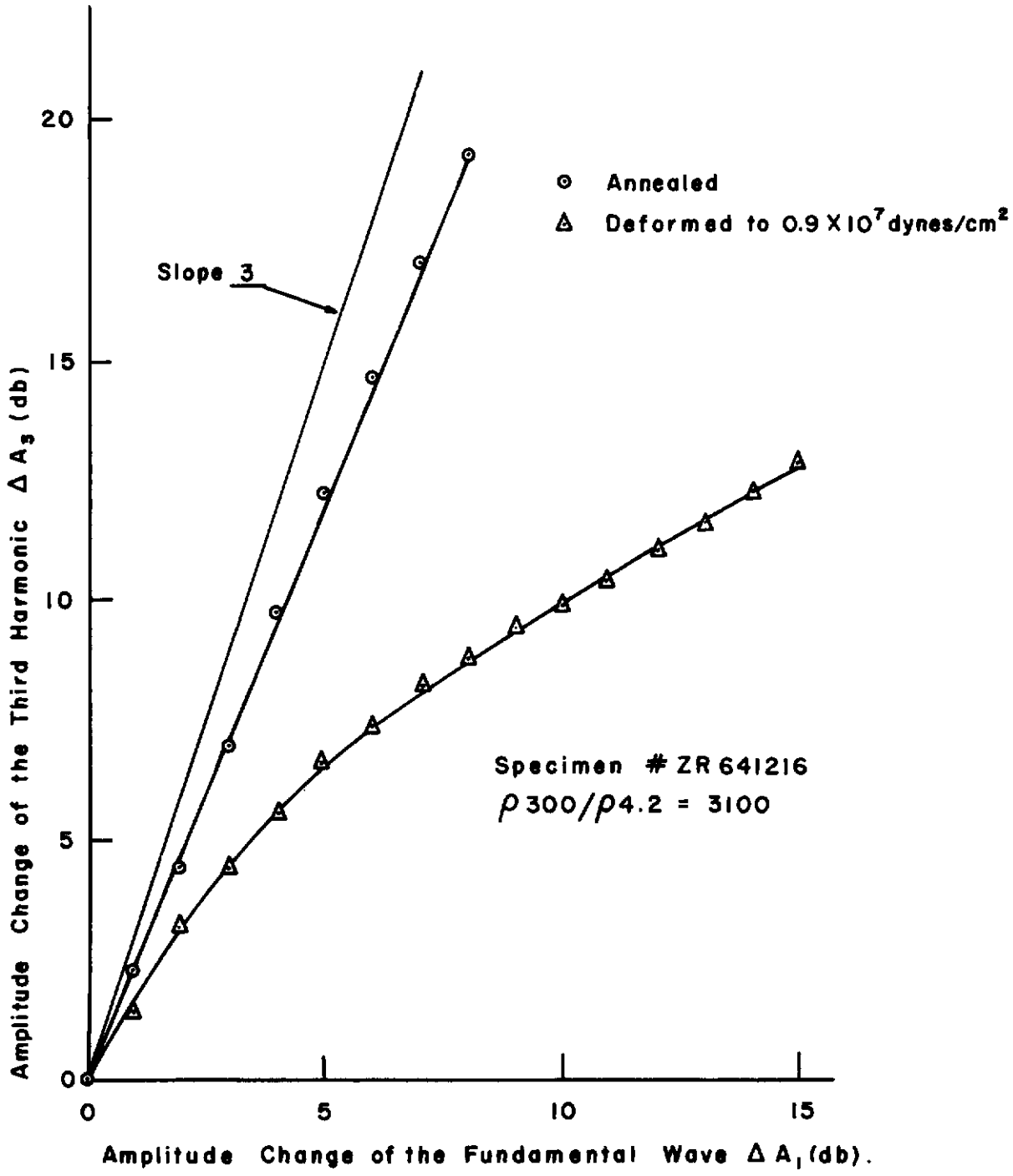

Figure 19. Effect of Plastic Deformation on the Amplitude of the Third Harmonic A_3.

for such attenuation are given in Equation (22) in which it is shown that α_1 is a function of A_1. In this expression for the attenuation α_1, derived on the basis of the nonlinear string model for dislocations, there are higher order terms, one of which has a dependence on A_1 through the amplitude of the second harmonic A_2, while another depends directly on A_1^2. Both quantities have a numerical value several orders of magnitude below the measured minimum detectable change in α_1 when reasonable values of L, B, and N are substituted. Thus, our results cannot be accounted for by the nonlinear string model behavior.

Next we consider the case in which the amplitude A_1 is sufficient to change the dislocation line length by an unpinning process. One type of unpinning process is a redistribution of pinners along the dislocation line that can be effected by an applied stress. This mechanism is treated by Alefeld[18] and Bauer[19]. Following Alefeld, the explanation for this phenomenon can be seen as follows: the driving force that results from an increase of the entropy of dislocations (which arises when the lengths of unpinned dislocation segments increase) tends to make pinning points group together. However, an equilibrium will be reached between the entropy increase due to long dislocation segments and the entropy decrease due to the grouping of pinning points. The application of a stress can upset this equilibrium and can change the distribution of pinners. The force component parallel to the dislocation line due to oscillatory stress is independent of the direction of the external stress and shifts the pinner towards the shorter line segment for positive as well as for negative stresses. Thus, the oscillatory stress field can create dislocation segments which are nearly free of pinning points. The conditions for the magnitude of dislocation line lengths and applied stress that are required for redistribution to take place are probably met in our experiment, but other aspects of the situation may make any redistribution negligible. In particular, if equilibrium thermodynamics are to prevail, we must assume that the frequency of oscillation is small compared with the reciprocal of the relaxation time, τ, for either the establishment of the new equilibrium distribution under stress or for the diffusion time of the pinners on the line. In our case this means that $\tau < \frac{1}{f} = 10^{-7}$ sec, and it is unlikely that any significant redistribution occurs in such a period.

A second type of unpinning involves the breakaway of dislocations from impurities. We consider first whether such a process is energetically possible under the conditions of the experiment. The binding energy of an impurity to an edge dislocation due to the hydrostatic pressure of the stress field is given by the following relation

$$U = A' \frac{\sin\theta}{r}$$

where θ and r are the polar coordinates of the impurity atom measured from the dislocation. It is expected that the solute atom is most strongly bound for the position $\theta = 3/2$ and for $r = 2 \times 10^{-8}$cm. Taking 0.1 ev for the strongest binding energy, A' is equal to 3.2×10^{-21}cm. ergs. The force binding the atom

is

$$F = -\frac{\partial U}{\partial r} = \frac{A'}{r^2} \simeq 10^{-5} \text{ dynes}$$

To determine the combination of applied stress and line length required to exert a force of this magnitude on the impurity, we use the term in the solution of the linear dislocation equation of motion that is due to a static stress σ_o:

$$\xi_o = \frac{4b\sigma_o}{C\pi} \frac{\ell^2}{\pi^2} \sin\frac{\pi\eta}{\ell}$$

The angle ϕ that the bowed out dislocation makes with the straight line equilibrium position (at the pinner, $\eta = 0$, see Figure 20) is determined by[7]

$$\left(\frac{\partial \xi_o}{\partial \eta}\right)_{\eta=o} = \frac{4b\sigma_o}{C\pi^2} \cdot \ell = \tan\phi$$

But the force on the impurity due to the bowed out dislocation segment on either side of it is given by

$$F = C\,(\sin\phi_1 + \sin\phi_2)$$

where C is the line tension of the dislocation. For small angles,

$$F = \frac{4b\sigma_o}{\pi^2}(\ell_1 + \ell_2)$$

and

$$\sigma_o = \frac{F\pi^2}{4b(\ell_1 + \ell_2)} = \frac{10^3}{\mathcal{L}}$$

where $\mathcal{L}$ is the critical breakaway length. Then a breakaway line length between 10^{-4} and 10^{-3}cm (a range likely to be found in our specimens) will require a stress of 10^6 to 10^7 dynes/cm^2 in the slip plane. The actual longitudinal stress required of course will be somewhat higher. Now according to our measurements the amplitude of the driving oscillatory wave is probably somewhat greater than 10^6 dynes/cm^2 at the driving transducer, indicating the possibility that there may be breakaway due to the stress of the ultrasonic wave.

Granato and Lücke[8] have discussed this type of mechanism extensively. In their treatment, the original exponential line length distribution derived by

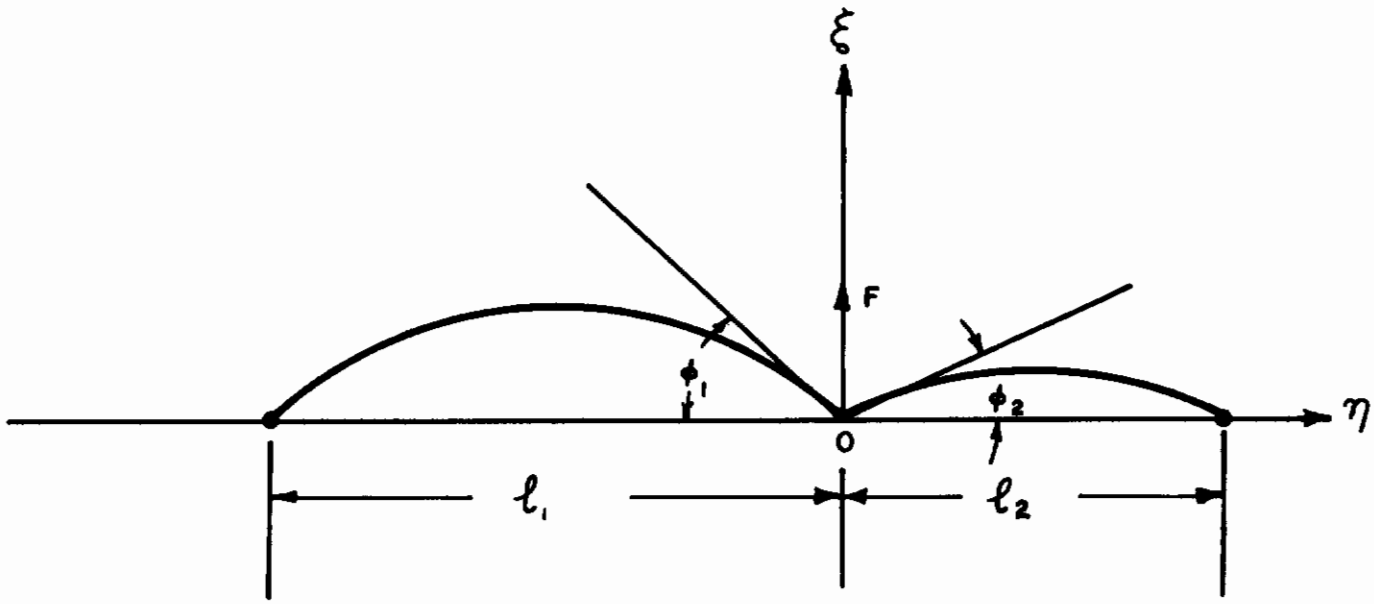

Figure 20. Force F acting on a pinning point at $\eta = 0$

Koehler[7] is modified to take into account the fact that the breakaway process is a catastrophic one within the network length. The distribution function is assumed to change from the initial exponential distribution at zero strain to a delta function distribution (all lengths having the same network length) when the strain is very large and all the loops have broken away. The distribution function is given by expression (51) in section III, which eventually leads to the expression for attenuation given by (72).

The existence of a distribution of loop lengths and an applied stress sufficient to cause breakaway can lead to two modes of vibration for dislocations: a string mode for lengths shorter than L and a hysteresis mode for lengths longer than L. For a very small applied stress no breakaway will take place, and there will be an exponential distribution of loop lengths, all the dislocations vibrating as strings that do not become unpinned during a stress cycle; for a larger stress all of the dislocations with $\ell < \mathcal{L}$ will vibrate in the string mode while those with $\ell > \mathcal{L}$ will vibrate in the hysteresis mode; finally, for a large enough stress, all the dislocations will break away and vibrate in the hysteresis mode.

Now we must examine the consequences of such behavior on the attenuation and on the third harmonic amplitude A_3. First, one must determine if the hysteresis loss is appreciable under the conditions of the experiment. Assuming that $L_n = 10^{-3}$cm, $L_c = 10^{-4}$cm, $N = 10^6$cm^{-2}, α_1 (Equation 72) becomes equal to 0.05 nepers/cm for a strain amplitude of $\varepsilon_o = 10^{-6}$. This result is of the order of magnitude of the maximum measured attenuation change that occurred as a result of changing A_1 by a factor of 10, that is, from a strain amplitude of about 10^{-7} to about 10^{-6}.

Now as pointed out previously, the process of plastic deformation leads to increased sensitivity in the attenuation changes observed when increasing A_1. See Figures 14, 16 and 18. When discussing the change of A_3 as a function of applied bias stress after plastic deformation, we concluded that the development of internal stress during work hardening could later make unpinning easier for the applied static bias stress. The same argument holds true for the oscillatory stress; after deformation, dislocation pile-ups increase the effectiveness of the stress wave in unpinning. However, since plastic deformation also increases the dislocation density, an increase in the change in attenuation due to an increase in strain amplitude may also be expected from this cause.

The interpretation of the data involving the measurement of A_3 as a function of A_1 is somewhat more difficult. First of all, Equation (77) predicts (on the basis of string model nonlinearity) that in the absence of any dislocation line length change and in the absence of any change in α_1 and α_3, the third harmonic amplitude should be proportional to the cube of the fundamental stress wave amplitude. (When A_1 and A_3 are plotted in db, the result should be a straight line of slope 3.) This is indeed the case for an annealed specimen of low resistivity ratio (R = 300), measurements on which are shown in Figure 15. For this experiment, we can assume that a relatively high density of impurities combined with the annealing process led to dislocation loop lengths so short that little or no unpinning occurred even when A_1 had the maximum value. The

extremely low change in α_1 as a function of A_1 for these conditions, shown in Figure 14, bears out this assumption.

However, in all the other experiments, involving samples of varying purity in annealed and deformed states, (Figures 15, 17 and 19) there is deviation from the line of slope 3. One must first determine if the measured change in α_1 with A_1 leads to a significant departure from the cubic power behavior. We substitute in the exponential factor of Equation (77), using for x the length of the specimen, the measured value of the third harmonic attenuation α_3, which is assumed not to be dependent on A_1, and the measured α_1 as a function of A_1. The result is that the magnitude of the deviation from the cubic power behavior is less than 10 percent of the observed value.

Next, one must examine the situation in which an increase in amplitude A_1 causes an increase in dislocation line length vibrating in the string mode, disregarding for a moment the effects of the associated hysteresis mode of vibration. In this view one may interpret the line length change entirely on the basis of the string model (Equation 77). Consider again the curve representing data on the deformed crystal shown in Figure 15. To discuss the deviation from the line of slope 3 we need to refer to the behavior of A_3 with applied bias stress as shown in Figure 11. These data were taken with A_1 at its maximum amplitude, that is, the same amplitude corresponding to +8 db on the abscissa of Figure 15. Since, for the deformed state, A_3 increases for low values of tensile bias stress, we concluded in the previous discussion that the average loop length is below ℓ_m as shown in the theoretical curve in Figure 9. According to the loop length dependence shown in Equation (77) then, a reduction in effective loop length, obtained for example by decreasing the amplitude of the fundamental wave, will further lower the amplitude of the third harmonic A_3. Thus, as A_1 is decreased from its maximum value, A_3 should decrease in proportion to the cube of A_1 as well as by some amount determined by the loop length function in Equation (77). This results in a slope greater than three and is contrary to the experimental evidence. The same contradiction is apparent in the data on the sample of intermediate purity (Figure 17) in the annealed state and after moderate deformation. Again, the third harmonic, when measured as a function of A_1, has a slope less than three, while the third harmonic measurements as a function of bias stress (Figure 12) indicate a loop length region such that the amplitude dependence should give a slope greater than three.

Qualitatively, however, the amplitude dependence of A_3 on A_1 may be explained in the case of the heavily deformed ⟨111⟩ sample (Figure 17) and the pure ⟨100⟩ sample (Figure 19). These specimens exhibit "overdamped" behavior in the bias stress experiments (Figures 12 and 13) indicating that the loop length change due to change in A_1 decreases the amplitude of the third harmonic so that a slope of less than 3 results in the experimental data.

It appears that the consequences of the string model vibration considered so far are insufficient to explain all of the amplitude dependent data. The hysteresis type dislocation behavior, shown to be a plausible mechanism in accounting for the amplitude dependent attenuation data, may well be a source of harmonic generation through the nonlinear stress strain relation associated with the break-

away process. Should the hysteresis mode be responsible for generating a third harmonic whose dependence on the amplitude of the fundamental involves a power less than three, the combination of a string mode mechanism and a hysteresis mode mechanism might lead to harmonic generation qualitatively consistent with the observations.

Absolute Measurements of Amplitude

In the studies carried out so far, good qualitative agreement was obtained between theoretical predictions and experimental results. One of the requirements for a quantitative check of the theory is an absolute measurement of the amplitudes. For this purpose a capacitive pick-up method described below was used.

Absolute amplitude measurements of 10 mc ultrasonic stress waves have been accomplished using a set-up indicated schematically in Figure 21. The method consists of measuring changes in the capacity of the condenser formed by the end of the specimen and a stationary plate, due to the displacement of the specimen end associated with the propagating wave (pulse).

For the conditions of the present experiment (see below for numerical values) the time constant of the circuit is approximately 10^{-4} sec. It is assumed, therefore, that for a wave with a frequency of 10 mc the stored charge remains constant during a cycle and thus any change in capacity, due to sample end displacement, manifests itself as a change in voltage across the gap. This voltage is amplified and measured with appropriate electronic circuitry. When the assumption of constant charge is valid, the relation between displacement d', gap width d, applied D.C. voltage V, and generated voltage V' is

$$d' = \frac{V'}{V} d \tag{78}$$

The electrical circuit for the capacitive pick-up is shown in Figure 22. The pick-up capacitor C_p formed by the end of the sample and the parallel pick-up electrode has various stray inductances and capacities associated with it. At 10 mc the inductances L_G and L_I may be neglected if the ground lead and input lead are kept reasonably short. Also $X_{cp} << R_g$ and $X_{cc} << X_{cx}$, R_g; therefore the circuit reduces to that shown in Figure 23.

The value of C_x may be measured by means of a bridge or "grid-dip" meter, where, for the components used in this circuit

$C_{stray} \approx 5$ pf, for socket and wiring

$C_{g,k+h} = 3.1$ pf, for 6922 vacuum tube

C_D = Dynamic input capacitance due to space charge which is normally 1/2 $C_{g,k+h}$

= 1.5 pf

$C_{Miller} = C_{gp}(1 + A)$ where A is the gain of the first triode and is equal to $\frac{\mu R_L}{R_L + r_p}$

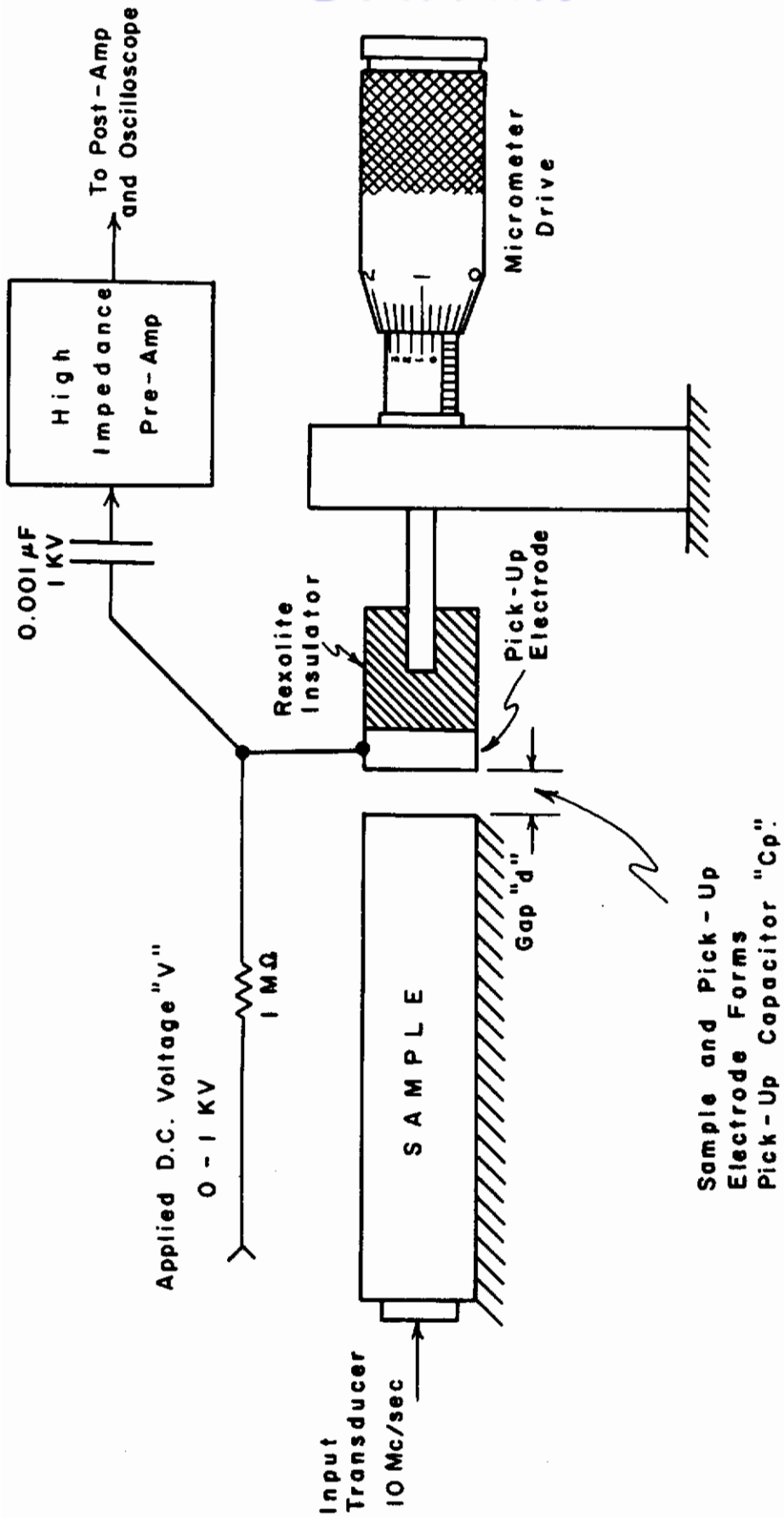

Figure 21. Experimental Arrangement for the Absolute Measurements of the Fundamental and Harmonic Waves.

approximately 1.8×10^{-7}cm. The round trip insertion loss in the sample was measured as 28 to 36 db (depending on the quality of the bond) so that the insertion loss from the input end to the capacitor pick-up end would be 14 to 18 db. Using a value for one way insertion loss of 16 db (or 6.3 to 1 ratio) would then indicate a displacement of $\pm 1.8 \times 10^{-7}/6.3 \cong \pm 2.9 \times 10^{-8}$cm at the pick-up end where the measured displacement with the capacitor was $\pm 3.5 \times 10^{-8}$cm. In view of the uncertainties in the insertion loss, the agreement between the calculated and measured displacement is considered reasonable and a test of the method for measuring the amplitude of the second and third harmonics was attempted.

The pick-up circuit used for this purpose is the same as that shown in Figure 22, except that the output of the cascode amplifier is tuned to the appropriate harmonic, and the input circuit reduces to that shown in Figure 23 if the inductances L_G and L_I can still be neglected. To verify whether these inductances are negligible, the resonant frequency of the entire input circuit was determined using a "grid-dip" meter. The value obtained was 150 mc. Since the pick-up capacitor C_p (63 pf) and the stray capacity C_x (12 pf) appear in series for this measurement, the total circuit capacity is calculated to be 10 pf. Then from the formula

$$L = \frac{1}{4\pi^2 f^2 C}$$

the total inductance is 0.011 microhenrys. The reactance of this value of inductance at 30 mc is 2.1 ohms and the reactance of C_x at 30 mc is 440 ohms, hence the inductance may be neglected in these measurements.

Before attempting to measure harmonic amplitude at 30 mc, the technique was verified by introducing a 30 mc stress wave into the sample and calculating the amplitude that should appear at the capacitor pick-up end. The peak-to-peak voltage applied to the 30 mc input transformer was 470 volts which produces a calculated unloaded displacement of the quartz transducer

$$u_{(0)} = 6.18 \times 10^{-8}\text{cm}.$$

The round trip insertion loss was measured as 32.6 db (11 volts peak to peak from first round trip echo). The one way insertion loss is then 16.3 db which corresponds to a factor of 6.53. Then the calculated displacement at the pick-up end is

$$u_{(\ell)\text{calc.}} = 6.18 \times 10^{-8}/6.53 = 9.4 \times 10^{-9}\text{cm}.$$

The measured value obtained with the pick-up capacitor was

$$u_{(\ell)} = 7.2 \times 10^{-9}\text{cm}.$$

The error between the two measurements is then

$$\frac{7.2 \times 10^{-9}}{9.4 \times 10^{-9}} = 0.765 = 24\%$$

Measurement of the third harmonic amplitude was then carried out by means of the pick-up capacitor and a value of

$$u_{3(\ell)meas.} = 4.35 \times 10^{-11} cm \ ,$$

which corresponds to a stress amplitude of

$$2.3 \times 10^{3} \ dynes/cm^{2} \ ,$$

was obtained when an input signal of 2800 volts (peak to peak) at 10 mc was applied to the input 10 mc quartz transducer. Since this applied voltage produces an unloaded displacement of

$$u_{(0)} = 3.31 \times 10^{-7} cm$$

and for this particular measurement the round trip insertion loss was measured as 28.5 db or a one-way loss of 14.25 db corresponding to a factor of 5.6, the calculated pick-up end displacement at 10 mc is

$$u_{(\ell)calc.} = 6.42 \times 10^{-8} cm$$

The ratio between the fundamental wave amplitude and the third harmonic amplitude at the pick-up end of the sample is simply

$$\frac{4.35 \times 10^{-11}}{6.42 \times 10^{-8}} = 0.678 \times 10^{-3}$$

or more than three orders of magnitude.

The amplitude of the third harmonic due to dislocations A_3 can be calculated from expression (77). If the following values are used

$\rho = 3 g/cm^{3}$, $\omega = 2\pi f = 6.28 \times 10^{7} \ sec^{-1}$, $k = \frac{\omega}{V} \cong 10^{+2} cm^{-1}$

$b = 3 \times 10^{-8} cm$, $A = \pi\rho b^{2} \cong 8 \times 10^{-15}$, $B = 4 \times 10^{-4}$ (estimated)

$C = \frac{\mu b^{2}}{2} \cong 10^{-4}$, $A_{10} = 4 \times 10^{6} \ dynes/cm^{2}$,

$\Omega R^{3} = 10^{-2}$ (estimated), $C' = 1$

N(effective dislocation density) $\cong 5 \times 10^{8} cm^{-2}$ (estimated),

one obtains for the value of the third harmonic amplitude

$$A_{3(calc)} \cong 3.2 \times 10^3 \text{ dynes/cm}^2$$

as compared to the measured value of

$$A_{3(meas.)} = 2.3 \times 10^3 \text{ dynes/cm}^2.$$

References

1) Technical Report AFML-TR-65-66, April, 1965

2) A. Hikata, B. B. Chick and C. Elbaum, Applied Phys. Letters 3, 195 (1963)

3) A. Hikata, B. B. Chick and C. Elbaum, J. Applied Phys. 36, 229 (1965)

4) J. M. Ziman, Electrons and Phonons, 152, Clarendon Press, 1960

5) T. Suzuki, A. Hikata and C. Elbaum, J. Applied Phys. 35, 2761 (1964)

6) L. D. Landau and E. M. Lifshitz, Theory of Elasticity, 115, Pergamon Press, (1959)

7) J. S. Koehler, Imperfections in Nearly Perfect Crystals, John Wiley & Sons, New York, (1952)

8) A. Granato and K. Lücke, J. Applied Phys. 27, 583 (1956)

9) R. M. Stern and A. Granato, Conference on Internal Friction, Acta Met. 10, 92 (1962)

10) A. J. E. Foreman, Acta Met. 3, 322 (1955)

11) G. deWit and J. S. Koehler, Phys. Rev. 116, 1113 (1959)

12) G. Leibfried, Oak Ridge Nat. Lab. Progr. Rep. No. ORNL 2829 (1959)

13) The displacement of the modes corresponding to n > 0 decreases very rapidly with increasing n and may be neglected for the purposes of this calculation.

14) When the term $\sin\frac{3\pi\eta}{L_o}$ is retained, various parts of the solution are multiplied by a numerical factor of order unity.

15) C. P. Bean, R. W. DeBlois and L. B. Nesbett, J. Applied Phys. 30, 1976 (1959)

16) A. Hikata, B. B. Chick, C. Elbaum and R. Truell, Acta Met. 10, 423 (1962)

17) A. H. Cottrell, Dislocations and Plastic Flow in Crystals, Oxford University Press, London (1953)

18) G. Alefeld, Phil. Mag. 11, 809 (1965)

19) C. L. Bauer, Phil. Mag. 11, 827 (1965)

List of Publications and oral presentations arising entirely or in part from the work on this Contract

Publications

A. Hikata, B. B. Chick and C. Elbaum, J. Applied Phys. 36, 229 (1965)

A. Hikata and C. Elbaum, Phys. Rev., in Press

Oral presentation

A. Hikata, F. Sewell and C. Elbaum, Am. Phys. Soc. Meeting, Washington, D. C., April 26, 1965

C. Elbaum, Symposium on Anharmonic Properties of Solids, Detroit, Michigan, October 18, 1965

A. Hikata, F. Sewell and C. Elbaum, Symposium on Anharmonic Properties of Solids, Detroit, Michigan, October 18, 1965

C. Elbaum, Meeting of the Acoustical Soc. Am., St. Louis, Missouri, November 4, 1965

C. Elbaum, ARPA Meeting, Providence, R. I., December 13, 1965

DOCUMENT CONTROL DATA - R&D

(Security classification of title, body of abstract and indexing annotation must be entered when the overall report is classified)

1. ORIGINATING ACTIVITY (Corporate author)	2a. REPORT SECURITY CLASSIFICATION
Brown University Providence, Rhode Island	UNCLASSIFIED
	2b. GROUP

3. REPORT TITLE

ULTRASONIC STUDIES OF THE NONLINEAR PROPERTIES AND OF THE DEFORMATION OF SOLIDS

4. DESCRIPTIVE NOTES (Type of report and inclusive dates)

Final Report - January 1, 1965 to December 31, 1965

5. AUTHOR(S) (Last name, first name, initial)

Hikata, Akira, Sewell, Frank A., Jr., Chick, Bruce B., and Elbaum, Charles

6. REPORT DATE	7a. TOTAL NO. OF PAGES	7b. NO. OF REFS
June 1966	79	7

8a. CONTRACT OR GRANT NO. AF 33(657)-8324	9a. ORIGINATOR'S REPORT NUMBER(S)
b. PROJECT NO. 7360	AFML-TR-65-56, Part II
c. TASK NO. 736002	9b. OTHER REPORT NO(S) (Any other numbers that may be assigned this report)
d.	

10. AVAILABILITY/LIMITATION NOTICES This document is subject to special export controls and each transmittal to foreign governments or foreign nationals may be made only with prior approval of the Metals and Ceramics Division (MAM), Air Force Materials Laboratory, Wright-Patterson AFB, Ohio.

11. SUPPLEMENTARY NOTES	12. SPONSORING MILITARY ACTIVITY
	Metals and Ceramics Division Air Force Materials Laboratory Wright-Patterson AFB, Ohio 45433

13. ABSTRACT

This report is concerned with a continuation (see report for 1964[1]) of the research on the nonlinear properties of solids, with special emphasis on the role of dislocations in harmonic generation, the effects of plastic deformation and dislocation interactions with point defects.

An expanded and improved theory of harmonic generation has been developed. The main new features of this theory include: 1) A demonstration that, in the string model, the nonlinear behavior of screw and edge dislocations is qualitatively and quantitatively different. In particular, it is shown that the nonlinear terms responsible for harmonic generation are of opposite sign for the two cases; edge dislocations behave as "hardening" strings and screw dislocations as "softening" strings. 2) The contributions of the lattice and of dislocations to the amplitude of the second harmonic are difficult to separate when the two are of comparable magnitude.

Dislocation breakaway from pinning points was considered as a possible source of harmonic generation; this contribution is of the same sign as that from screw dislocations.

DD FORM 1 JAN 64 1473

14. KEY WORDS	LINK A		LINK B		LINK C	
	ROLE	WT	ROLE	WT	ROLE	WT

INSTRUCTIONS

1. ORIGINATING ACTIVITY: Enter the name and address of the contractor, subcontractor, grantee, Department of Defense activity or other organization *(corporate author)* issuing the report.

2a. REPORT SECURITY CLASSIFICATION: Enter the overall security classification of the report. Indicate whether "Restricted Data" is included. Marking is to be in accordance with appropriate security regulations.

2b. GROUP: Automatic downgrading is specified in DoD Directive 5200.10 and Armed Forces Industrial Manual. Enter the group number. Also, when applicable, show that optional markings have been used for Group 3 and Group 4 as authorized.

3. REPORT TITLE: Enter the complete report title in all capital letters. Titles in all cases should be unclassified. If a meaningful title cannot be selected without classification, show title classification in all capitals in parenthesis immediately following the title.

4. DESCRIPTIVE NOTES: If appropriate, enter the type of report, e.g., interim, progress, summary, annual, or final. Give the inclusive dates when a specific reporting period is covered.

5. AUTHOR(S): Enter the name(s) of author(s) as shown on or in the report. Enter last name, first name, middle initial. If military, show rank and branch of service. The name of the principal author is an absolute minimum requirement.

6. REPORT DATE: Enter the date of the report as day, month, year; or month, year. If more than one date appears on the report, use date of publication.

7a. TOTAL NUMBER OF PAGES: The total page count should follow normal pagination procedures, i.e., enter the number of pages containing information.

7b. NUMBER OF REFERENCES: Enter the total number of references cited in the report.

8a. CONTRACT OR GRANT NUMBER: If appropriate, enter the applicable number of the contract or grant under which the report was written.

8b, 8c, & 8d. PROJECT NUMBER: Enter the appropriate military department identification, such as project number, subproject number, system numbers, task number, etc.

9a. ORIGINATOR'S REPORT NUMBER(S): Enter the official report number by which the document will be identified and controlled by the originating activity. This number must be unique to this report.

9b. OTHER REPORT NUMBER(S): If the report has been assigned any other report numbers *(either by the originator or by the sponsor)*, also enter this number(s).

10. AVAILABILITY/LIMITATION NOTICES: Enter any limitations on further dissemination of the report, other than those imposed by security classification, using standard statements such as:

(1) "Qualified requesters may obtain copies of this report from DDC."

(2) "Foreign announcement and dissemination of this report by DDC is not authorized."

(3) "U. S. Government agencies may obtain copies of this report directly from DDC. Other qualified DDC users shall request through _____."

(4) "U. S. military agencies may obtain copies of this report directly from DDC. Other qualified users shall request through _____."

(5) "All distribution of this report is controlled. Qualified DDC users shall request through _____."

If the report has been furnished to the Office of Technical Services, Department of Commerce, for sale to the public, indicate this fact and enter the price, if known.

11. SUPPLEMENTARY NOTES: Use for additional explanatory notes.

12. SPONSORING MILITARY ACTIVITY: Enter the name of the departmental project office or laboratory sponsoring *(paying for)* the research and development. Include address.

13. ABSTRACT: Enter an abstract giving a brief and factual summary of the document indicative of the report, even though it may also appear elsewhere in the body of the technical report. If additional space is required, a continuation sheet shall be attached.

It is highly desirable that the abstract of classified reports be unclassified. Each paragraph of the abstract shall end with an indication of the military security classification of the information in the paragraph, represented as *(TS), (S), (C), or (U)*.

There is no limitation on the length of the abstract. However, the suggested length is from 150 to 225 words.

14. KEY WORDS: Key words are technically meaningful terms or short phrases that characterize a report and may be used as index entries for cataloging the report. Key words must be selected so that no security classification is required. Identifiers, such as equipment model designation, trade name, military project code name, geographic location, may be used as key words but will be followed by an indication of technical context. The assignment of links, rules, and weights is optional.

Experiments were carried out on aluminum single crystals with several different impurity contents, as measured by electrical resistivity ratios ($R_{300°K}/R_{4.2K}$) ranging from 270 to 3100. Amplitudes of the third harmonic, as well as the attenuation of the fundamental wave, were measured as a function of bias stress, amplitude of the fundamental wave and amount of plastic deformation. The results of these experiments are consistent with the qualitative predictions of the theory presented.

A capacitive pick-up method was used to measure the magnitude of the fundamental and higher harmonic amplitudes for the purpose of comparison with the quantitative aspects of the theory.